Compositional Characteristics of Fluvial Particulate Organic Matter Exported From the World's Largest Alpine Wetland

Guohua Dai[1], Erxiong Zhu[1,2], Zongguang Liu[1,2], Yiyun Wang[1,2], Shanshan Zhu[1,2], Simin Wang[1,2], Tian Ma[1,2], Juan Jia[1,2], Xin Wang[1,2], Shengjie Hou[3], Pingqing Fu[2,3] (iD), Francien Peterse[4] (iD), and Xiaojuan Feng[1,2] (iD)

[1]State Key Laboratory of Vegetation and Environmental Change, Institute of Botany, Chinese Academy of Sciences, Beijing, China, [2]College of Resources and Environment, University of Chinese Academy of Sciences, Beijing, China, [3]State Key Laboratory of Atmospheric Boundary Layer Physics and Atmospheric Chemistry, Institute of Atmospheric Physics, Chinese Academy of Sciences, Beijing, China, [4]Department of Earth Sciences, Utrecht University, Utrecht, Netherlands

Abstract Wetlands are hot spots for particulate organic matter (POM) supply into rivers, which link the land-ocean transfer in the global carbon cycle. However, the source, composition, and seasonal variability of POM carried by wetland-draining rivers are poorly constrained. Here we combine bulk and source-specific biomarker analyses to investigate the fluvial POM biogeochemistry of the Black and White Rivers draining from the Zoige wetland. We find that POM was dominated by terrestrial organic matter including high-molecular-weight (HMW) lipids, branched glycerol dialkyl glycerol tetraethers, and lignin phenols. However, fluvial POM was rich in HMW lipids and poor in lignin phenols compared to the catchment soils, possibly due to hydrodynamic sorting and dissolution processes. While lignin phenol concentrations were higher in the wet season, HMW lipid concentrations were lower. Additionally, lignin phenols increased with total suspended solids, while HMW lipids decrease. These contrasts imply an enhanced input of lignin-rich particles from soil surface layers in the wet season, diluting HMW lipids. Compared with that in other rivers around the world with a higher forest coverage in the catchment, POM in the Black and White Rivers draining grass-dominated wetlands had a much higher ratio of HMW fatty acids to lignin phenols. Our results represent a benchmark study highlighting compositional characteristics of fluvial POM exported from the Zoige wetland and the divergent behavior of molecular components during fluvial transfer. Such information is vital for assessing future changes in the Zoige wetland, given its high vulnerability to climatic and land use changes.

1. Introduction

Fluvial transport of particulate organic matter (POM) is a crucial link between terrestrial and marine systems in global biogeochemical cycles (Cole et al., 2007; Galy et al., 2015; Schlünz & Schneider, 2000). Globally, POM makes up about half of the total organic carbon (OC) flux (0.40 Pg C/year) from rivers to the ocean, with a significant fraction buried in marine sediments (Galy et al., 2015; Schlünz & Schneider, 2000). The source and lability of the transported and buried POM are closely related to its impacts on the atmospheric CO_2 levels and long-term climate regulation (Galy et al., 2015; Ward et al., 2013). Hence, understanding the sources and composition of POM transported by rivers is important to assess its impact of fluvial transport on regional and global carbon cycles (Freymond et al., 2018; Galy et al., 2015; Hedges et al., 1986).

Wetlands, usually drained by streams and rivers, are key sources of POM to rivers due to their huge organic matter storage and eroding potentials (Cole et al., 2007; Limpens et al., 2008; McClelland et al., 2016). Furthermore, widespread increases in particulate organic carbon (POC) fluxes have been observed in rivers draining peatlands in past decades due to climatic changes (e.g., warming, drying, and elevated CO_2) and land use changes (e.g., drainage, overgrazing, and peat extraction; Regnier et al., 2013; McClelland et al., 2016), suggesting enhanced fluvial POM export from wetlands in the future. However, the sources, composition, and fate of POM in these wetland-draining rivers are still poorly examined. Filling the knowledge gap will help us better understand the nature of carbon exported from wetlands as well as the effects of climate and environmental change on fluvial carbon export (Feng et al., 2013; Pawson et al., 2008).

Fluvial POM consists of a complex mixture of compounds from different terrestrial and aquatic sources with different physical/chemical behaviors and recalcitrance toward decomposition (Feng et al., 2013; Freymond et al., 2018; Ward et al., 2013; Worrall et al., 2017). Source-specific biomarkers are useful tools for tracing various POM components in aquatic ecosystems (Hedges et al., 1986; Spencer et al., 2016; Tesi et al., 2014). In particular, lignin-derived phenols that have a high abundance in vascular plant tissues (~30%; reviewed by Thevenot et al., 2010) are recently shown to predominantly trace organic matter sourced from surface pools within the Arctic watersheds due to their high abudance in surface organic matter, whereas plant wax lipids may track organic matter liberated from deeper soils due to their relative enrichment in the mineral horizons and tendency to associate with fine particles (Feng et al., 2013; Feng, Gustafsson, Holmes, Vonk, van Dongen, Semiletov, Dudarev, Yunker, Macdonald, Wacker, et al., 2015). In addition, emergent biomarkers such as isoprenoid and branched glycerol dialkyl glycerol tetraethers (iGDGTs and brGDGTs), which are membrane lipids mainly derived from archaea and bacteria, respectively, have been increasingly used to distinguish inputs from aquatic versus soil environments (Schouten et al., 2013, and references therein). Hence, these different groups of biomarkers have the potential to disentangle and compare the inputs and fate of organic matter sourced from contrasting carbon pools during land-river transfer. However, although the abovementioned biomarkers have been extensively employed and studied in large rivers (e.g., Hemingway et al., 2017; Spencer et al., 2016; van Dongen et al., 2008), their behavior and seasonal variations in small rivers draining wetland-dominated watersheds are less well known. Compared with upland soils in large river basins, wetland soils are often water saturated and experience relatively small moisture changes throughout the year. We hence expect compositional differences in fluvial POM in wetland- versus upland-draining rivers resulting from varied soil organic matter composition in oxic and anoxic soils, such as a better preservation of lipids in wetland soils due to thermodynamic constraints on the anaerobic decomposition of reduced compounds (Keiluweit et al., 2017). Seasonal variations in the composition of POM may be smaller in wetland- than in upland-draining rivers due to relatively consistent hydrological pathways in the former watersheds. However, POM signals stemming from small river basins may also be more responsive to hydrological changes compared with large catchments whose signals are smoothed out. Hence, it remains to be investigated how POM composition varies in small rivers mainly draining wetlands relative to the well-investigated large rivers.

Here we investigate the sources and composition of POM in two main rivers draining the Zoige wetland, the world's largest alpine wetland located in northeastern Qinghai-Tibetan Plateau. Ongoing climate change and human disturbances have led to severe degradation of the Zoige wetland over the past decades (Ma et al., 2016; Yang et al., 2017) and may accelerate carbon cycling and enhance carbon export in the future, either directly to the atmosphere or indirectly to the drainage system, thereby changing the carbon sink strength of the Zoige wetland. Several studies have highlighted the increased release of CO_2 and methane from the Zoige wetland in response to wetland degradation over the past 40 years (Yang et al., 2017; Zhou et al., 2015). However, investigations on the fluvial export of OC from the region are currently sparse (Zhu et al., 2014). The Zoige wetland, drained by two rivers with contrasting bedrock and organic matter content (i.e., the Black and White Rivers), has a high potential for POM release via fluvial export. However, the composition and quantity of exported POM remains unknown. In this study, we analyze multiple source-specific biomarkers (including wax lipids, iGDGTs, brGDGTs, and lignin phenols) in POM collected from the Black and White Rivers during the wet and dry seasons to (1) characterize the sources and composition of riverine POM in comparison with catchment soils; (2) characterize seasonal variations and controls on POM composition as a benchmark study for the Zoige wetland; and (3) compare the molecular characteristics of POM exported from wetland-dominated catchments with those from other rivers around the world.

2. Materials and Methods

2.1. Study Area and Sampling

The Zoige wetland (101°36′–103°55′E, 32°20′–34°05′N), covering 1.2×10^4 km² on the northeastern part of Qinghai-Tibetan Plateau with an average altitude of 3,500m above sea level, is the largest alpine wetland in the world (Gao et al., 2014). Mean annual temperature in this region is ~1 °C, while mean annual precipitation averages at 690 mm, 90% of which falls between June and September. Vegetation in the Zoige wetland is dominated by nonwoody species such as *Carex muliensis*, *Polygonum aviculare*, *Elymus*

dahuricus, *Potentilla anserina*, and *Caltha palustris* (Gao et al., 2014; Li, Chen, et al., 2018). Soils mainly include Leptosols, Histosols, and Cryosols according to the International Union of Soil Sciences Working Group World Reference Base (2015) for Soil Resources and are estimated to contain 1.1 Pg of soil organic carbon (SOC) to the depth of 1 m (Ma et al., 2016), accounting for 6.2% of SOC storage in China.

The Black and White Rivers are important tributaries in the upper reaches of the Yellow River (Figure 1) and are the two major rivers that originate from and flow through the Zoige wetland. The Black River is ~500 km long and drains an area of 7,600 km^2, and the White River is ~270 km long and drains an area of 5,500 km^2. Peatland covers 29% and 10% of the Black and White River catchments, respectively (Zhu et al., 2014), giving the Black River water a darker color compared with the White River. The hydrological regimes of both rivers are characterized by a monomodal hydrogram with high- and low-water phases, occurring in June–August and in September–May, respectively (Annual Hydrological Report P.R. China, 2015; Wang et al., 2010). From November to March, both rivers are almost entirely ice covered. Despite the high elevation of the catchment, snow accumulation is not very strong due to low precipitation in the winter. Hence, flooding mainly occurs in the summer instead of spring. Two sampling campaigns were conducted in July 2015 and April 2016. The July sampling campaign corresponds to the high-water (wet) season of the Black (discharge to mean discharge ratio; $Q/Q_{mean} = 3.19$) and White Rivers ($Q/Q_{mean} = 3.01$), while the April campaign corresponds to the low-water (dry) season ($Q/Q_{mean} = 0.45$ and 0.55 for the Black and White Rivers, respectively). The wet-season discharge was 64.4 and 175 m^3/s for the Black (at Dashui gauging station) and White (at Tangke gauging station) Rivers, respectively, and the dry-season discharge was 10.5 and 30.2 m^3/s (Annual Hydrological Report P.R. China, 2015).

River samples were collected at nine stations along the Black River and seven stations along the White River during both sampling campaigns (Figure 1). Samples were collected between 10 a.m. and 4 p.m. on four consecutive days from different stations. No rain occurred during sampling. Surface water was collected from the middle of the river at each site using high-density polyethylene containers that were cleaned with soapy water and then soaked with 10% HCl solution for 24 hr and rinsed with Milli-Q water three times before use. The precleaned containers were rinsed three times with river water prior to sampling. For every sampling site, triplicate water samples were collected and mixed in equal proportions in situ to constitute a single representative sample. Total suspended solid (TSS) was determined by filtering a known volume of water (100−300 ml) through a precombusted, preweighed Whatman GF/F filter (47 mm, 0.7 μm) at each site on the day of sampling. The filters were freeze-dried using a SCANVAC CoolSafe^{TM} (model 110-4, LaboGene^{TM}, Lynge, Denmark) freeze-dryer (the same type throughout this paper) and weighed to determine the TSS concentration (mg/L). Water temperature, pH, dissolved oxygen, and conductivity were measured in situ using a portable WTW (Multi 3420) multiparameter meter.

For POM analysis, large volumes of surface water (>10 L in the wet season and >25 L in the dry season) were collected at each site. To prevent bacterial and algal growth, 200 μl of saturated $HgCl_2$ solution was added per liter of water. Suspended particles were allowed to settle in the dark at ambient temperature (~15 °C). After 2 days, the supernatant was decanted and filtered onto precombusted (550 °C, 4 hr), preweighed glass fiber filters (Whatman GF/F, 0.7 μm). The mass of particles retained on the filters was determined by weighing after freeze-drying. The settled particles were recovered, freeze-dried, weighed, and stored frozen (–20 °C) until analyses. Compared with particles retained on the glass filters, the settled particles represent >90% of TSS at all sites and showed similar composition with TSS that was directly filtered in situ according to our preliminary tests. As TSS was difficult to retrieve from glass filters for subsequent lignin analysis (which uses hot alkaline solutions that dissolve glass), we used the settled particles to represent POM in this study.

In addition to river samples, soils were collected in July 2015 from three representative sites within each of the Black and White River catchments (Figure 1). At every site, three random soil cores were collected using a stainless steel gravity corer (diameter of 5 cm) from each of three random quadrats (0.5 m × 0.5 m) at the depths of 0−10, 10−20, 20−30, 30−50, and 50−70 cm. The three soil cores from the same depth and quadrant were mixed, homogenized in equal proportions as one composite sample, and passed through a 2-mm sieve to remove stones and visible roots. Soil samples were then stored frozen in precleaned high-density polyethylene bottles in the dark until being freeze-dried before analysis. Given the tedious analysis of biomarkers, we selected three depths that correspond to the commonly referred surface (0−10 cm), subsurface (20−30 cm), and deep (50−70 cm) soils for further analyses in this study. Although the sampling
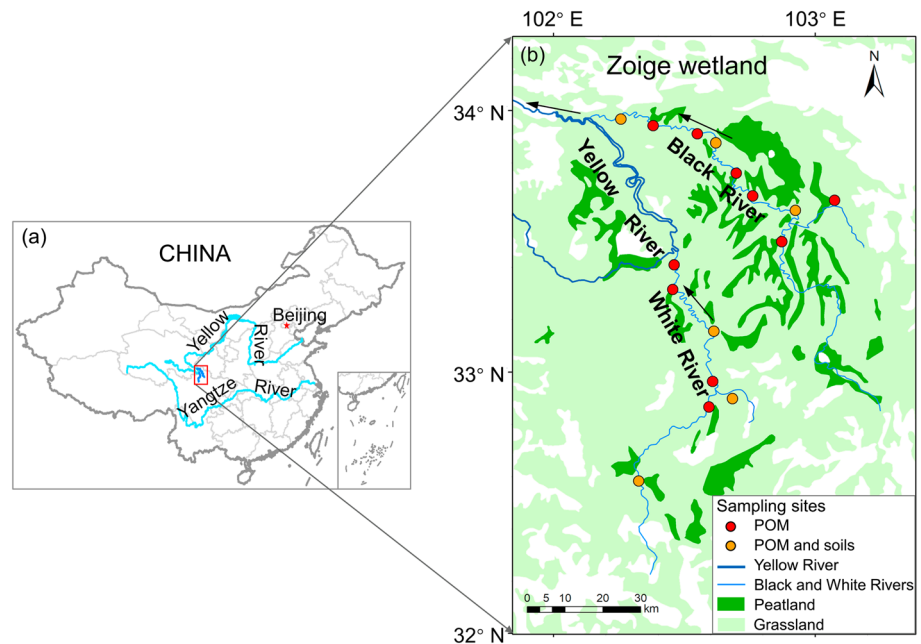
Figure 1. (a) Location of the Black and White Rivers in the Zoige wetland and (b) sampling sites along the rivers underlain by peatland. Peatland cover is derived from China's vegetation map (1:1,000,000). Arrows indicate river flow direction. POM = particulate organic matter.

density is relatively low, these samples serve our purpose of revealing compositional contrasts between riverine POM and soil, which are strong enough to override spatial and depth variabilities of biomarker concentrations previously analyzed across a regional-scale transect on the Qinghai-Tibetan Plateau (Dai et al., 2018; Ma et al., 2019; Zhu et al., 2019).

2.2. Elemental and Isotopic Analyses

Riverine POM (i.e., the settled particles) and soil samples were decarbonated by fumigation using 12 M hydrochloric acid (HCl) for 72 hr with the excessive HCl vapor subsequently removed by sorbing to sodium hydroxide pellets under vacuum for 24 hr. Samples were then dried in an oven for 24 hr at 60 °C. The contents of POC, particulate nitrogen (PN), SOC, and soil nitrogen (SN) were measured using a Flash 2000 Organic Elemental Analyzer. Analytical precision (standard deviation for repeated measurements of internal standards) was $\pm 0.4\%$ for carbon and $\pm 1.0\%$ for nitrogen. POC or PN concentrations (mg/L) were calculated as the product of POC or PN content (%) and POM concentrations in water (mg/L). The stable isotopes of carbon and nitrogen were measured for POM ($\delta^{13}C$ and $\delta^{15}N$) using an elemental analyzer coupled with isotope ratio mass spectrometer (MS; DELTAplus, Thermo Finnigan MAT 253, Germany). The precision was $\pm 0.1\%_0$ and $\pm 0.2\%_0$ for $\delta^{13}C$ and $\delta^{15}N$, respectively. The DOC concentrations of filtered surface waters (<0.7 μm) were measured using the Multi N/C 3100 analyzer (Analytik Jena, Germany).

2.3. Biomarker analyses

Strict quality control was ensured for biomarker analyses. Solvents were all high-performance liquid chromatograph grade and purchased from Dikma Technologies (USA). All glassware was rinsed with dichloromethane and methanol before use. Procedural blanks containing no sample but only solvents were processed and analyzed in the same way for every 20 samples. Procedural blanks, solvent blanks, and external quantification standards were analyzed on the same instruments for every batch of samples to ensure the absence of contamination and to check the response of instruments. Duplicates of samples were also analyzed to ensure the reproducibility of results.

2.3.1. Wax Lipids

Wax lipids were isolated from freeze-dried POM (0.25−0.35 g) or soils (5−8 g) by sonication (15 min) with 30 ml of dichloromethane, dichloromethane:methanol (1:1, v:v), and methanol (Otto & Simpson, 2005).

The total lipid extracts were filtered through precombusted glass fiber filters (Whatman GF/F) and evaporated to almost dryness. After the addition of an internal standard (C_{19} n-alkanoic acid; 100 μl, 0.11 μg/μl), the extracts were redissolved to 1 ml with dichloromethane:methanol (1:1, v:v). Quantitative aliquots (100−300 μl) of the extracts were dried under nitrogen gas (N_2) and converted to trimethylsilyl (TMS) derivatives by reacting with 40 μl of N,O-bis-(trimethylsilyl)trifluoroacetamide, 10 μl of pyridine, and 50 μl dichloromethane for 3 hr at 70 °C. Compounds were identified and quantified on a Thermo TRACE 1310 gas chromatograph (GC) coupled to an ISQ MS (Thermo Fisher Scientific, USA) using a DB-5MS column (30 m × 0.25 mm inner diameter; film thickness 0.25 μm) for separation. The temperature increased from 65 °C (initial hold time 2 min) to 300 °C at a rate of 6 °C/min with helium as the carrier gas (1.2 ml/min). The injection temperature was fixed at 280 °C, and the extracts (1 μl) was injected in the splitless mode. The MS was operated in the electron impact mode with ionization energy of 70 eV and scanned from 50 to 650 Da. The ion source and interface temperatures were set at 280 and 250 °C, respectively. GC-MS data were acquired and processed using the Xcalibur software. Quantification was achieved by comparison of peak areas of individual compounds with the internal standard (C_{19} n-alkanoic acid-TMS) in the total ion current. External standards (including C_{18} n-alkane, C_{19} n-alkanoic acid-TMS, C_{19} n-alkanol-TMS, and 5α-cholestane) were used to normalize the response factor for different lipid classes relative to C_{19} n-alkanoic acid (TMS). The concentrations of n-alkanes, n-alkanols, and steroids were reevaluated according to the response ratios of C_{18} n-alkane, C_{19} n-alkanol, and 5α-cholestane to C_{19} n-alkanoic acid, which were 0.62, 0.65, and 0.73, respectively. Analytical errors were typically <10% based on three replicate analysis of the same sample.

A series of n-alkanoic acids or fatty acids (FAs), n-alkanols, n-alkanes, and steroids are major classes of compounds found in the wax lipid extracts of both POM and soil samples analyzed. Diagnostic indices based on wax lipids have been used to trace the origin and behavior of POM or sediments in aquatic ecosystems (Bianchi & Canuel, 2011; Ficken et al., 2000). Among these, carbon preference index (CPI), the terrestrial-to-aquatic ratio (TAR), and the proportion of aquatic components (P_{aq}) of n-alkanes are most frequently used (Ficken et al., 2000; Jaffé et al., 1995; van Dongen et al., 2008) with calculations shown in the following equations:

$$CPI = 0.5 \times \left(\frac{C_{25} + C_{27} + C_{29} + C_{31} + C_{33}}{C_{24} + C_{26} + C_{28} + C_{30} + C_{32}} + \frac{C_{25} + C_{27} + C_{29} + C_{31} + C_{33}}{C_{26} + C_{28} + C_{30} + C_{32} + C_{34}} \right) \quad (1)$$

where C_n is the relative abundance of n-alkanes with n number of carbon atoms (the same hereinafter). Usually, CPI > 5 indicates the dominance of terrestrial sources (Bianchi & Canuel, 2011; Cranwell et al., 1987), and the CPI value decreases with progressive degradation (Otto & Simpson, 2005; Wiesenberg et al., 2010).

$$P_{aq} = (C_{23} + C_{25})/(C_{23} + C_{25} + C_{29} + C_{31}) \quad (2)$$

P_{aq} indicates the relative inputs of submerged/floating aquatic macrophytes versus emergent and terrestrial plants. For modern plants, $P_{aq} < 0.1$ corresponds to terrestrial plants, 0.1–0.4 to emergent macrophytes, and 0.4–1.0 to submerged/floating macrophytes (Ficken et al., 2000).

$$TAR = (C_{27} + C_{29} + C_{31})/(C_{15} + C_{17} + C_{19}) \quad (3)$$

TAR has been widely used as a proxy for assessing the relative contributions of terrestrial and aquatic lipids in aquatic environments. Generally, TAR > 1 indicates terrestrial sources, while TAR < 1 indicates aquatic sources (Bianchi & Canuel, 2011; van Dongen et al., 2008).

2.3.2. Glycerol dialkyl glycerol tetraethers

After wax lipid analysis, the remaining total lipid extracts (700−900 μl out of 1 ml) were kept at −20 °C before being separated into two fractions using a silica gel column (0.5-cm inner diameter; 7 cm in length) by sequential elution with hexane:dichloromethane (9:1, v:v; 10 ml; apolar fraction) and dichloromethane:methanol (1:1, v:v; 10−15 ml; polar fraction), respectively (Schouten et al., 2013). Glycerol dialkyl glycerol tetraethers (GDGTs), present in the polar fraction, were kept frozen until analyzed for both POM and soil samples at Utrecht University. Briefly, 99 ng of an internal C_{46} GDGT standard dissolved in mixture of

hexane:isopropanol (99:1, *v:v*) was added to the polar fraction for quantification, dried under N_2, redissolved in hexane:isopropanol (99:1, *v:v*), and filtered through 0.45-μm polytetrafluoroethylene filters. This internal standard with two glycerol head groups linked by a C_{20} alkyl chain and two C_{10} alkyl chains was initially synthesized by Patwardhan and Thompson (1999) and tested as an internal standard by Huguet et al. (2006). Compounds were analyzed using an Agilent 1260 ultrahigh-performance liquid chromatograph (UHPLC) coupled to an Agilent 6310 quadrupole MS with atmospheric pressure chemical ionization. The separation of GDGTs was achieved with an improved chromatography method to detect both 5-methyl and 6-methyl brGDGTs (De Jonge et al., 2014; Hopmans et al., 2016). Briefly, separation was achieved by two silica Waters Acquity UHPLC ethylene-bridged hybrid (BEH) hydrophilic interaction chromatography (HILIC) columns (150 × 2.1 mm, 1.7 μm) at 30 °C, with a guard column (7.5 × 2.1 mm, 5 μm) of the same material preceding both. An injection volume of 10 μl and a flow rate of 0.2 ml/min were used. Samples were eluted with 82% hexane and 18% hexane:isopropanol (9:1, *v:v*) for 25 min, followed by a linear gradient to 70% hexane, 30% hexane:isopropanol (9:1, *v:v*) for 25 min, and then to 100% hexane:isopropanol (9:1, *v:v*) in 30 min. Quantification was achieved in selected ion monitoring (SIM) mode using *m/z* 1,292, 1,302, 1,300, 1,298, and 1,296 for iGDGTs; *m/z* 1,050, 1,048, 1,046, 1,036, 1,034, 1,032, 1,022, 1,020, and 1,018 for brGDGTs; and *m/z* 744 for the internal standard (Figure S1 in the supporting information; Huguet et al., 2006; Dang et al., 2016).

The brGDGTs included three series (I, II, and III; Figure S1) according to their degree of methylation, with each series including components with 0–2 cyclopentyl rings (e.g., Ia, Ib, and Ic). The iGDGTs included GDGT 0−3, crenarchaeol, and crenarchaeol′. GDGT-based proxies were calculated using the following equations, in which roman numbers refer to the relative abundance of GDGT structures (Figure S1) and 6-methyl brGDGT isomers are indicated with a′. The branched and isoprenoid tetraether (BIT) index is an estimate of the relative abundance of major bacterial brGDGTs representing terrestrial organic matter and a specific iGDGT, crenarchaeol, representing aquatic organic matter. The BIT index can reach values theoretically ranging from 0 to 1, representing a purely aquatic or a soil source of the OC, respectively (Hopmans et al., 2004):

$$BIT = \frac{Ia + IIa + IIIa + IIa' + IIIa'}{Ia + IIa + IIIa + IIa' + IIIa' + \text{crenarchaeol}} \tag{4}$$

The relative amounts of the pentamethylated and hexamethylated 6-methyl brGDGTs compared to the total pentamethylated and hexamethylated brGDGTs are expressed as the isomer ratio (IR), which is thought to be an indicator of aquatic brGDGT production (De Jonge et al., 2014):

$$IR = \frac{IIa' + IIb' + IIc' + IIIa' + IIIb' + IIIc'}{IIa + IIb + IIc + IIIa + IIIb + IIIc + IIa' + IIb' + IIc' + IIIa' + IIIb' + IIIc'} \tag{5}$$

The modified cyclisation of branched tetraethers (CBT′) and methylation of branched tetraethers (MBT$'_{5ME}$) indices were calculated (De Jonge et al., 2014):

$$CBT' = \frac{Ic + IIa' + IIb' + IIc' + IIIa' + IIIb' + IIIc'}{Ia + IIa + IIIa} \tag{6}$$

$$MBT'_{5ME} = \frac{Ia + Ib + Ic}{Ia + Ib + Ic + IIa + IIb + IIc + IIIa} \tag{7}$$

Additionally, the ratio of GDGT-0/crenarchaeol was calculated, where GDGT-0/crenarchaeol > 2 is generally thought to indicate a substantial methanogenic contribution for GDGT-0 (Blaga et al., 2009).

2.3.3. Lignin Phenols

Lignin-derived phenols were released from the dried solvent-extracted residues using the alkaline copper oxide (CuO) oxidation method (Feng, Gustafsson, Holmes, Vonk, van Dongen, Semiletov, Dudarev, Yunker, Macdonald, Montluçon, et al., 2015). Briefly, ~0.2 g of POM or 1- to 2-g soil residues were mixed with 0.5- to 1-g CuO, 80- to 100-mg ammonium iron (II) sulfate hexahydrate [Fe $(NH_4)_2(SO_4)_2 \cdot 6H_2O$],

and 20 ml of N_2-purged sodium hydroxide solution (2 M) in Teflon-lined bombs. All bombs were flushed with N_2 in the headspace for 10 min and heated at 170 °C for 2.5 hr. The oxidation products were spiked with a recovery standard (ethyl vanillin), acidified to pH 1 with 12 M HCl, and kept in the dark for 1 hr. After centrifugation (2,500 rpm for 10 min), oxidation products were liquid-liquid extracted from the clear supernatant with ethyl acetate three times, spiked with an internal standard (*trans*-cinnamic acid), and concentrated under N_2 for further analysis. Quantification of the oxidation products was conducted on a Thermo TRACE 1310 GC-ISQ-MS, with the same derivatization method and GC-MS operating conditions as for wax lipids. Phenols were identified by comparing the mass spectra with the authentic standards of all typical lignin phenols and MS libraries. Quantification was achieved by comparing with recovery standards (ethyl vanillin) to account for compound loss during extraction procedures. External quantification standards were used to normalize the response factor for different lignin phenols. The coefficient of variation associated with phenol concentrations are typically <10% based on three replicate analysis of the same sample.

Lignin concentrations refer to the summed concentrations of eight lignin monomers, including the universal and most abundant vanillyl phenols [V; vanillin (Vl), acetovanillone (Vn), vanillic acid (Vd)], angiosperm-specific syringyl phenols [S; syringaldehyde (Sl), acetosyringone (Sn), syringic acid (Sd)], and cinnamyl phenols (C; *p*-coumaric acid, ferulic acid) found in nonwoody tissues. Additionally, CuO oxidation also releases *p*-hydroxy (P) phenols [including *p*-hydroxybenzoic acid, *p*-hydroxybenzaldehyde, and *p*-hydroxyacetophenone (Pn)] and 3,5-dihydroxybenzoic acid (3,5Bd) that may derive from protein and "tannin-like" compounds and/or demethylation of lignin (Feng, Gustafsson, Holmes, Vonk, van Dongen, Semiletov, Dudarev, Yunker, Macdonald, Montluçon, et al., 2015; Goni & Hedges, 1995). In particular, it is found that P phenols (especially Pn) are enriched in *Sphagnum* (Amon et al., 2012; Tesi et al., 2014), while 3,5Bd is most enriched in soil/peat and may indicate brown macroalgae (e.g., kelp) in marine environments (Bianchi & Canuel, 2011; Feng, Gustafsson, Holmes, Vonk, van Dongen, Semiletov, Dudarev, Yunker, Macdonald, Montluçon, et al., 2015).

Ratios of S/V and C/V are used to indicate the relative input of angiosperm and nonwoody tissues versus gymnosperm wood, respectively (Goni & Hedges, 1995; Thevenot et al., 2010). Both ratios have also been observed to decrease with the preferential degradation of S and C relative to V phenols (Thevenot et al., 2010, and references therein). The ratio of Pn/P is used to assess the influence of *Sphagnum* as the ratio is relatively high in mosses and peat (Pn/P = 0.84; Amon et al., 2012; Feng, Gustafsson, Holmes, Vonk, van Dongen, Semiletov, Dudarev, Yunker, Macdonald, Montluçon, et al., 2015; Tesi et al., 2014). Additionally, the ratio of P/V may reflect the decomposition due to demethylation of V phenols, when the other sources of P phenols (such as protein) are relatively constant (Ellis et al., 2012; Feng, Gustafsson, Holmes, Vonk, van Dongen, Semiletov, Dudarev, Yunker, Macdonald, Montluçon, et al., 2015). By comparison, the ratio of 3,5Bd/V is usually considered to reflect organic matter transformation in soils or sediments as plants allegedly contain very low abundance of 3,5Bd (Bianchi & Canuel, 2011, and references therein). The acid-to-aldehyde (Ad/Al) ratios of V and S phenols are widely used to indicate lignin degradation and increases with increasing lignin oxidation (Goni & Hedges, 1995; Hedges et al., 1986).

2.4. Statistical Analyses

Shapiro-Wilk and Levene tests were performed for all variables to check the normal distribution of data and homogeneity of variance, respectively. Nonparametric tests (Mann-Whitney *U* or Kruskal-Wallis) were conducted if data were not normally distributed (even after log or square-root transformation), while *T* tests or one-way analysis of variance was conducted for normally distributed data. Specifically, the independent-sample *T* tests were used to determine differences of variables between two seasons or rivers, whereas the one-way analysis of variance (followed by Games-Howell test for the non-homogeneous variables) was used to determine differences among three soil layers or varied sample types (i.e., wet- and dry-season POM and soils). Pearson correlation was used to determine relationships between normally distributed variables, while Spearman linear correlation was used for non-normally distributed variables (i.e., TSS, low-molecular-weight [LMW] lipids, and brGDGTs). Differences and correlations were considered to be significant at a level of $p < 0.05$.

3. Results

3.1. Bulk Properties of Soils and River Water

Soils had similar SOC, SN contents, and SOC/SN ratios in the catchments of the Black and White Rivers (except SOC at the 0−10 cm; $p > 0.05$; $n = 9$; Table S1). The above parameters decreased with depths in the White River catchment ($p < 0.05$; $n = 3$), but the trend was not significant in the Black River catchment. Both the Black and White Rivers had a higher temperature, higher dissolved oxygen contents, and higher conductivity in the wet (July) than in the dry (April) season ($p < 0.05$; $n = 9$ in the Black and 7 in the White Rivers for POM bulk properties throughout this paper; Table 1), with the latter reflecting increased concentration of solutes due to increased soil erosion in the wet season (Ihejirika et al., 2011). The pH of river water was slightly more acidic during the wet season in the Black River ($p < 0.05$; $n = 9$; Table 1), possibly due to increased leaching of acidic peat. In comparison, the White River has a much smaller coverage of peatland in its basin and therefore is less influenced (Zhu et al., 2014). In addition, both rivers had higher TSS, POC, and PN concentrations (in mg/L) and atomic ratios of POC to PN (POC/PN_a), and lower DOC/POC ratios in the wet than in the dry season ($p < 0.05$; Table 1). The ratio of DOC/POC was lower in the Black (0.62 ± 0.09; $n = 18$) than in the White River (2.17 ± 0.68; $n = 14$) in both seasons ($p < 0.05$; Table 1). No significant difference was found among sampling sites for any of the above parameters in either river.

3.2. Wax Lipids in the POM and Soils

FAs and n-alkanols were dominated by even-numbered homologues in the range of $C_{24}−C_{30}$, while n-alkanes were dominated by odd-numbered homologues in the range of $C_{23}−C_{33}$ in both soils and riverine POM. Among the identified steroids (β-sitosterol, campesterol, stigmasterol, stigmasta-3,5-dien-7-one, sitosterone, and ergosterol), β-sitosterol was the most abundant in all samples. The identified wax lipids were grouped into three categories according to their sources. The first class, high-molecular-weight (HMW) lipids exclusively derived from terrestrial plants, included even-numbered FAs ($C_{24}−C_{32}$) and n-alkanols ($C_{24}−C_{32}$), odd-numbered n-alkanes ($C_{27}−C_{31}$), and steroids (other than ergosterol). The second class, low-molecular-weight (LMW) lipids occurring in both aquatic and terrestrial sources (including algae, bacteria, and plants), included short-chain ($<C_{20}$) FAs, n-alkanols and n-alkanes, and ergosterol (Bianchi & Canuel, 2011; Otto & Simpson, 2005). The third class, midchain lipids, included C_{20} and C_{22} FAs and n-alkanols, and C_{21}, C_{23}, and C_{25} n-alkanes that may derive from submerged/floating aquatic macrophytes in aquatic environment (Bianchi & Canuel, 2011). However, due to their minor contribution (~10%) to total identified wax lipids and invariant concentrations between seasons in either river, they were excluded from further analyses.

In the catchment soils, HMW lipids accounted for $53\% \pm 2\%$ of the total identified wax lipids. Both HMW and LMW lipids were slightly more concentrated in the soils of the Black than in the White River basin ($p < 0.05$; $n = 9$; Figure 2a). Concentrations of HMW and LMW lipids and the associated geochemical parameters (e.g., CPI and P_{aq}) showed no significant difference with soil depth in either river basin ($p > 0.05$; $n = 3$; Figures 3a and S2). In the riverine POM, wax lipids had a much higher OC-normalized concentration than that in soils ($p < 0.05$; Table S2). HMW lipids also accounted for $55\% \pm 2\%$ of the total identified wax lipids. HMW and LMW lipids had slightly lower OC-normalized concentrations in the POM of the Black than of the White River ($p < 0.05$; $n = 18$ and 14 in the Black and White Rivers, respectively; Figure 2b). Temporally, both HMW and LMW lipids had higher concentrations in the dry than in the wet season in the Black River ($p < 0.05$; $n = 9$; Figure 2c). In the White River, LMW lipids showed higher concentrations in the dry than in the wet season ($p < 0.05$; $n = 7$; Figure 2d), while HMW lipids showed the opposite temporal trend ($p < 0.05$; $n = 7$). In addition, both CPI and P_{aq} were comparable between the Black and White Rivers ($p > 0.05$; $n = 18$ and 14 in the Black and White Rivers, respectively; Figure 3a and Table S2), while TAR showed higher values in the Black than in the White River ($p < 0.05$). Temporally, the CPI values were higher in the wet than in the dry season in both rivers ($p < 0.05$). No seasonal differences were found for the TAR or P_{aq} values ($p > 0.05$). POM had higher values of P_{aq} than had soils for the respective basins ($p < 0.05$), while CPI was comparable between soils and the dry-season POM in both rivers (Table S2).

3.3. GDGTs in the POM and Soils

In the catchment soils, brGDGTs accounted for $78\% \pm 3\%$ of total GDGTs (Table S2). The brGDGTs consisted mostly of 5-methyl brGDGTs (Ia, Ib, Ic, IIa, IIb, and IIIa; Figures S3a–S3c). The iGDGTs in soils were

Table 1
Bulk Properties of Surface Waters and Particulate Organic Matter From the Black and White Rivers During the Wet and Dry Seasons (Mean ± Standard Error)

Parameter	Black River		White River	
	Wet season ($n = 9$)	Dry season ($n = 9$)	Wet season ($n = 7$)	Dry season ($n = 7$)
Water temperature (°C)	14.7 ± 0.7 a	11.9 ± 0.5 b	15.7 ± 0.8 A	11.4 ± 0.7 B
Water pH[a]	6.9–8.2 b	7.3–8.2 a	7.6–7.8 A	7.1–8.2 A
DO (mg/L)	4.56 ± 0.13 a	2.28 ± 0.05 b	4.90 ± 0.13 A	2.55 ± 0.06 B
Conductivity (μm/S)	244 ± 51 a	186 ± 16 a	241 ± 56 A	131 ± 7 B
TSS (mg/L)	455.6 ± 60.2 a	192.7 ± 12.7 b	243.9 ± 52.8 A	32.9 ± 12.0 B
DOC (mg/L)	7.04 ± 0.41 a	7.13 ± 0.48 a	4.52 ± 0.47 A	2.87 ± 0.37 B
POC (mg/L)	21.68 ± 2.88 a	9.26 ± 1.07 b	8.85 ± 1.30 A	1.33 ± 0.45 B
POC (%)	4.79 ± 0.17 a	4.75 ± 0.46 a	3.97 ± 0.33 A	4.50 ± 0.47 A
PN (mg/L)	1.50 ± 0.20 a	0.67 ± 0.07 b	0.60 ± 0.09 A	0.10 ± 0.03 B
PN (%)	0.33 ± 0.01 a	0.34 ± 0.03 a	0.27 ± 0.02 A	0.35 ± 0.04 A
POC/PN$_a$	16.9 ± 0.3 a	15.9 ± 0.3 b	17.2 ± 0.2 A	15.2 ± 0.3 B
$\delta^{13}C$ (‰)	−26.26 ± 0.04 a	−26.39 ± 0.06 a	−26.50 ± 0.07 A	−26.38 ± 0.06 A
$\delta^{15}N$ (‰)	2.38 ± 0.13 a	2.57 ± 0.10 a	2.08 ± 0.09 A	2.45 ± 0.18 A
DOC/POC	0.37 ± 0.05 b	0.88 ± 0.13 a	0.55 ± 0.06 B	3.80 ± 1.06 A

Note. Different letters indicate significant differences between the wet and dry seasons for the Black (lowercase letters) and White (uppercase letters) Rivers, respectively ($p < 0.05$). DO = dissolved oxygen; TSS = total suspended solid; DOC = dissolved organic carbon; POC = particulate organic carbon; PN = particulate nitrogen; POC/PN$_a$ = the atomic ratio of POC to PN; DOC/POC = the ratio of DOC to POC.
[a]Ranges are shown for surface water pH values because the pH scale is logarithmic.
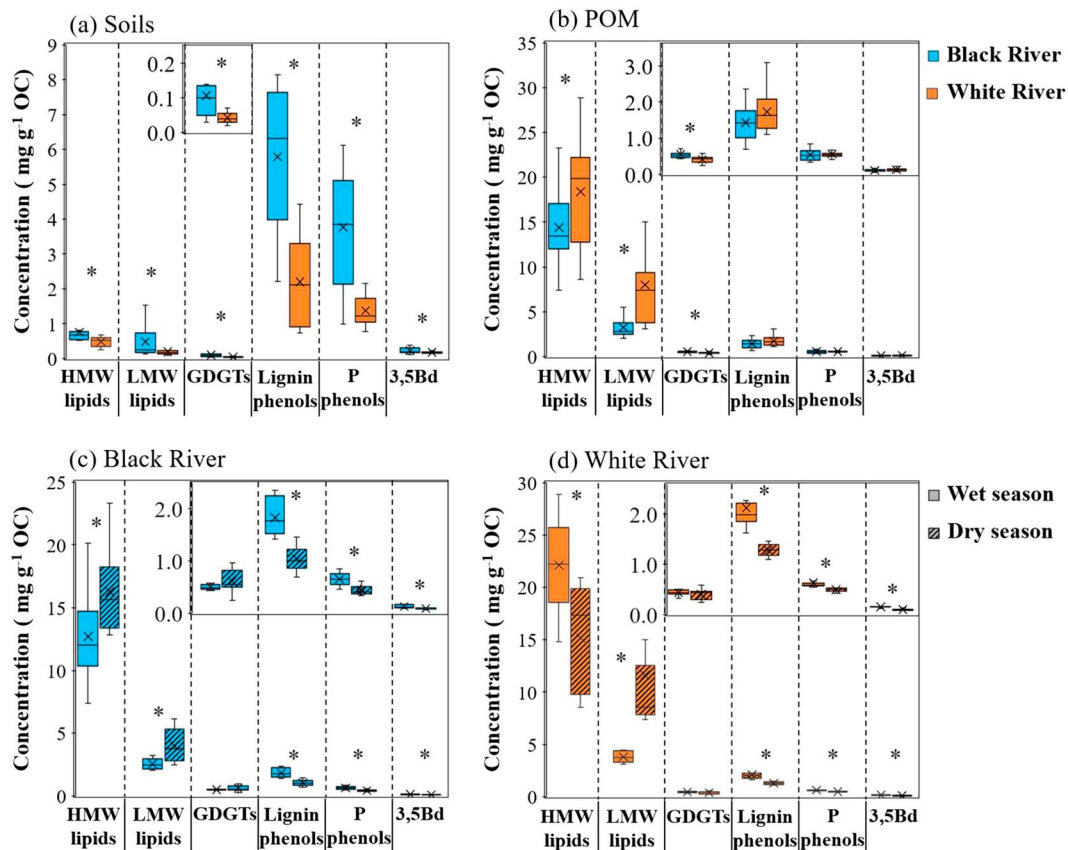

Figure 2. Organic carbon (OC)-normalized concentrations of biomarkers in the (a) catchment soils and (b) riverine particulate organic matter (POM) of the (c) Black and (d) White Rivers as an average of seasons and during the wet and dry seasons. The solid bar and cross in the box mark the median and mean of each data set, respectively. The upper and lower ends of boxes denote the 0.25 and 0.75 percentiles, respectively. Asterisks indicate differences between rivers and between seasons ($p < 0.05$). HMW = high-molecular-weight; LMW = low-molecular-weight; GDGTs = glycerol dialkyl glycerol tetraethers, including branched and isoprenoid GDGTs; P phenols = *p*-hydroxyl phenols; 3,5Bd: 3,5-dihydroxybenzoic acid.
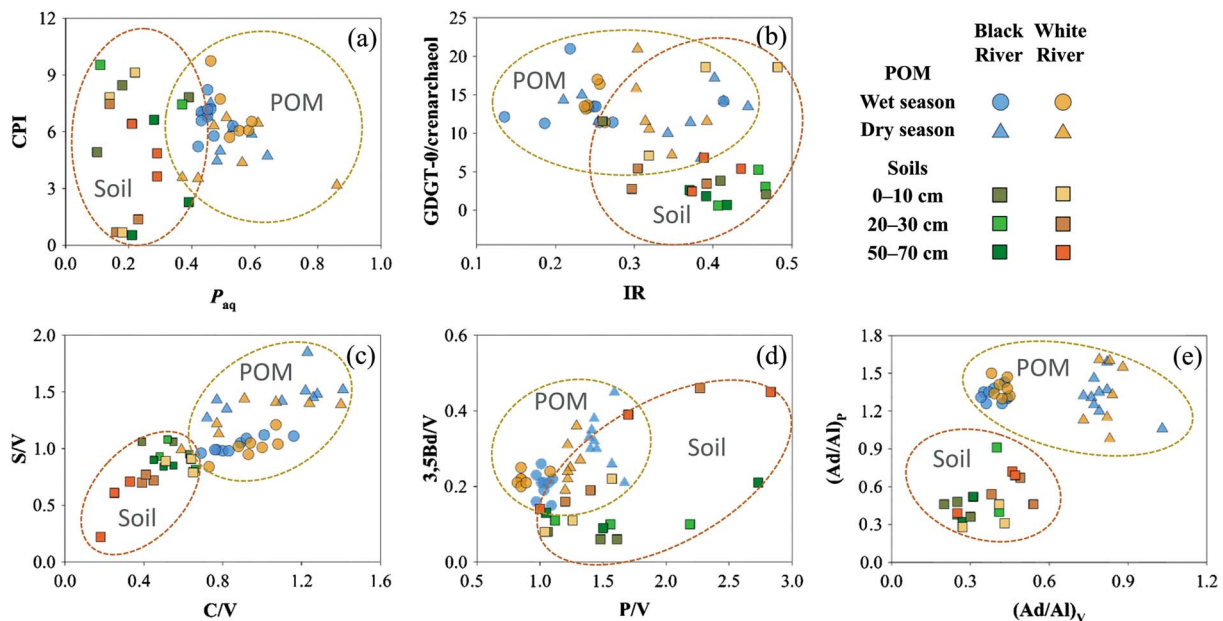
Figure 3. Biomarker-related indicators in riverine particulate organic matter (POM) and soil samples. CPI, P_{aq}, and IR proxies are defined in Equations 1, 2, and 5. CPI = carbon preference index of *n*-alkanes; P_{aq} = proportion of aquatic *n*-alkanes; IR = isomer ratio of branched glycerol dialkyl glycerol tetraethers; V = vanillyl phenols; S = syringyl phenols; C = cinnamyl phenols; P = *p*-hydroxy phenols; 3,5Bd = 3,5-dihydroxybenzoic acid; $(Ad/Al)_V$ and $(Ad/Al)_P$ = the acid-to-aldehyde ratio of V and P phenols, respectively. GDGT-0/crenarchaeol ratio of >2 is generally thought to indicate a substantial methanogenic origin for GDGT-0 (Blaga et al., 2009).

dominated by GDGT-0 (31–94% of iGDGTs; Figures S3b–S3d), followed by crenarchaeol. The average ratio of GDGT-0/crenarchaeol (5.7 ± 1.3; Table S2) was higher than 2. The BIT values were high in soils (0.80−0.98). Almost all GDGT-related parameters, including BIT, CBT′, IR, and GDGT-0/crenarchaeol were comparable between the two basins ($p > 0.05$; $n = 9$). Notably, MBT'_{5ME} showed higher ratios in the White River basin soils, caused by the higher fractional abundances of brGDGT IIb and IIIa ($p < 0.05$; $n = 9$; Table S2 and Figure S3c). Overall, both brGDGT and iGDGT concentrations and the associated geochemical parameters showed no significant variation with soil depth in either river basin ($p > 0.05$; $n = 3$; Figures 3b and S2).

Similar to wax lipids, GDGTs were more concentrated relative to bulk OC in the riverine POM than in soils ($p < 0.05$; Table S2). Both brGDGTs and iGDGTs were more abundant in the Black than in the White River POM per unit of OC ($p < 0.05$; $n = 18$ and 14 in the Black and White Rivers, respectively; Table S2 and Figure 2b). GDGTs in the POM were dominated by brGDGTs ($88.6\% \pm 0.32\%$ of total GDGTs), in line with previous observations based on riverine POM and sediments (Li et al., 2015; Naeher et al., 2014; van Dongen et al., 2008). BrGDGTs in the POM were dominated by 5-methyl brGDGTs (63–85% of total brGDGTs; Table S2), while iGDGTs were dominated by GDGT-0 (75–87% of total iGDGTs). The GDGT-0/crenarchaeol ratio (6.8–21) and BIT values (0.98−1.0) were higher in the riverine POM than in the soils of the catchments ($p < 0.05$; Table S2), while MBT'_{5ME} values (0.19−0.37) were lower in the riverine POM ($p < 0.05$). Dry-season POM had similar values of IR and CBT′ as soils in the respective basins (Table S2). Temporally, both brGDGT and iGDGT concentrations and GDGT-related proxies (including BIT, MBT'_{5ME}, and GDGT-0/crenarchaeol) had no variation between seasons in either river ($p > 0.05$; Figures 2c and 2d and Table S2), while the IR and CBT′ values in both rivers were slightly higher in the dry than in the wet season ($p < 0.05$; Figure 3b and Table S2).

3.4. Lignin Phenols in the POM and Soils

Lignin and P phenols had higher OC-normalized concentrations in the soils of the Black than of the White River basin ($p < 0.05$; $n = 9$; Figure 2a). Lignin-related source and degradation indicators were comparable between basins ($p > 0.05$; $n = 9$). The C/V ratio decreased with increasing soil depths in the White River

basin ($p < 0.05$; $n = 3$), whereas all other parameters and phenol concentrations showed no significant variation with soil depth in either river basin ($p > 0.05$; Figure S2 and Table S2). Unlike wax lipids and GDGTs, the analyzed phenols were less abundant relative to the bulk OC in the riverine POM than in the soils of the respective basins (except for lignin phenols and 3,5Bd in the wet-season POM of the White River; $p < 0.05$; Table S2). Only the P/V ratio showed higher ratios in the Black than in the White River ($p < 0.05$; $n = 18$ and 14 in the Black and White Rivers, respectively; Figure 3d). Temporally, lignin phenols, P phenols, and 3,5Bd all had higher concentrations in the wet than in the dry season in both rivers ($p < 0.05$; Figures 2c and 2d), while ratios of S/V, P/V, $(Ad/Al)_V$, and 3,5Bd/V in both rivers and C/V in the Black River were higher in the dry than in the wet season ($p < 0.05$; Table S2). The ratio of Pn/P was higher in the wet than in the dry season in both rivers ($p < 0.05$). Ratios of $(Ad/Al)_S$ and $(Ad/Al)_P$ showed no seasonal variations in either river ($p > 0.05$). Ratios of C/V and $(Ad/Al)_P$ were higher in the POM than in the soils of both basins ($p < 0.05$), while all other parameters showed no obvious patterns.

3.5. Relationships of Biomarker Distributions With Water and POM Properties in Rivers

The relationships of biomarker distributions with river water and POM properties in the Black and White Rivers were determined by Pearson correlation (or Spearman correlation for relationships involving TSS and LMW lipids) for the original data (Figure 4). Among the investigated parameters, POC and PN concentrations are significantly correlated with TSS ($r > 0.9$; $p < 0.001$; $n = 18$ and 14 in the Black and White Rivers, respectively) and thus are excluded to avoid redundancy. Similarly, both P phenols and 3,5Bd showed a strong correlation with lignin phenols ($r > 0.8$; $p < 0.001$; $n = 18$ and 14 in the Black and White Rivers, respectively) and were thus excluded in the correlation analysis. HMW lipids are only negatively correlated to TSS concentrations in the Black River ($r = -0.50$; $p = 0.04$; $n = 18$) but are positively correlated to POC/PN_a ($r = 0.60$; $p = 0.03$; $n = 14$) and negatively correlated to $\delta^{15}N$ in the White River ($r = -0.62$; $p = 0.03$; $n = 14$). LMW lipids are negatively correlated to TSS ($r = -0.87$; $p < 0.001$; $n = 18$ in the Black River; and $r = -0.73$; $p = 0.001$; $n = 14$ in the White River; Figure 4) and POC/PN_a ($r = -0.81$; $p = 0.001$; $n = 18$, and $r = -0.52$; $p = 0.03$; $n = 14$ in the Black and White Rivers, respectively) in both rivers and are also positively correlated to $\delta^{15}N$ in the Black River ($r = 0.50$; $p = 0.04$; $n = 18$). By comparison, lignin phenols are positively correlated to TSS ($r = 0.61$; $p = 0.03$; $n = 18$ in the Black River; and $r = 0.67$; $p = 0.002$; $n = 14$ in the White River) and POC/PN_a ($r = 0.85$; $p < 0.001$; $n = 18$, and $r = 0.70$; $p = 0.002$; $n = 14$ in the Black and White Rivers, respectively) and are negatively correlated to $\delta^{15}N$ in both rivers ($r = -0.70$; $p = 0.01$; $n = 18$, and $r = -0.58$; $p = 0.01$; $n = 14$). The abundances of both brGDGTs and iGDGTs are not influenced by any river water and POM properties, except for iGDGTs being negatively correlated to $\delta^{13}C$ of POM in the Black River ($r = -0.52$; $p = 0.03$; $n = 18$).

4. Discussion

4.1. Sources and Composition of Riverine POM in Comparison With Soils

Similar to that in other rivers with a high coverage of wetland in their basins (such as Russian Arctic rivers (van Dongen et al., 2008), Harney River in Florida Everglades (Jaffé et al., 2006), and five tributaries of Lake Pääjärvi, southern Finland (Huotari et al., 2013)), POM in the Black and White Rivers flowing through the Zoige wetland was dominated by terrestrial organic matter. This is indicated by (i) high POC/PN_a ratios (14.1−18.2) and depleted POM $\delta^{13}C$ and $\delta^{15}N$ values (Table 1) similar to those in terrestrial plant tissues from Zoige wetland (Gao et al., 2014; Li, Chen, et al., 2018) but significantly lower than those in autochthonous sources from Zoige wetland ($\delta^{13}C$ of −16.07‰ to −24.11‰, $\delta^{15}N$ of 4.45−7.28‰; Li, Chen, et al., 2018); (ii) high abundance of higher plant-derived HMW lipids and lignin phenols (Table S2); and (iii) biomarker-based geochemical indicators. For instance, riverine POM had a BIT index of 0.98−1.0, close to the theoretical end-member value for soils (~1) (Hopmans et al., 2004; Schouten et al., 2013). The proportion of 6-methyl brGDGTs has recently been suggested to indicate potential in situ production of brGDGTs in riverine POM or sediments (reflected by high values of IR and CBT′; De Jonge et al., 2014). However, in the Black and White Rivers, both IR and CBT′ were comparable or even lower in the POM than that in catchment soils (Figure 3b), supporting a predominant terrestrial origin of brGDGTs in both rivers. In addition, the higher ratio of GDGT-0/crenarchaeol in the POM than in the catchment soils (Table S2) is driven by a relatively low abundance of crenarchaeol in POM, confirming a minor aquatic GDGT contribution. Similarly, the average CPI (6.1 ± 0.3) and TAR values (>10) of n-alkanes in our study were comparable to
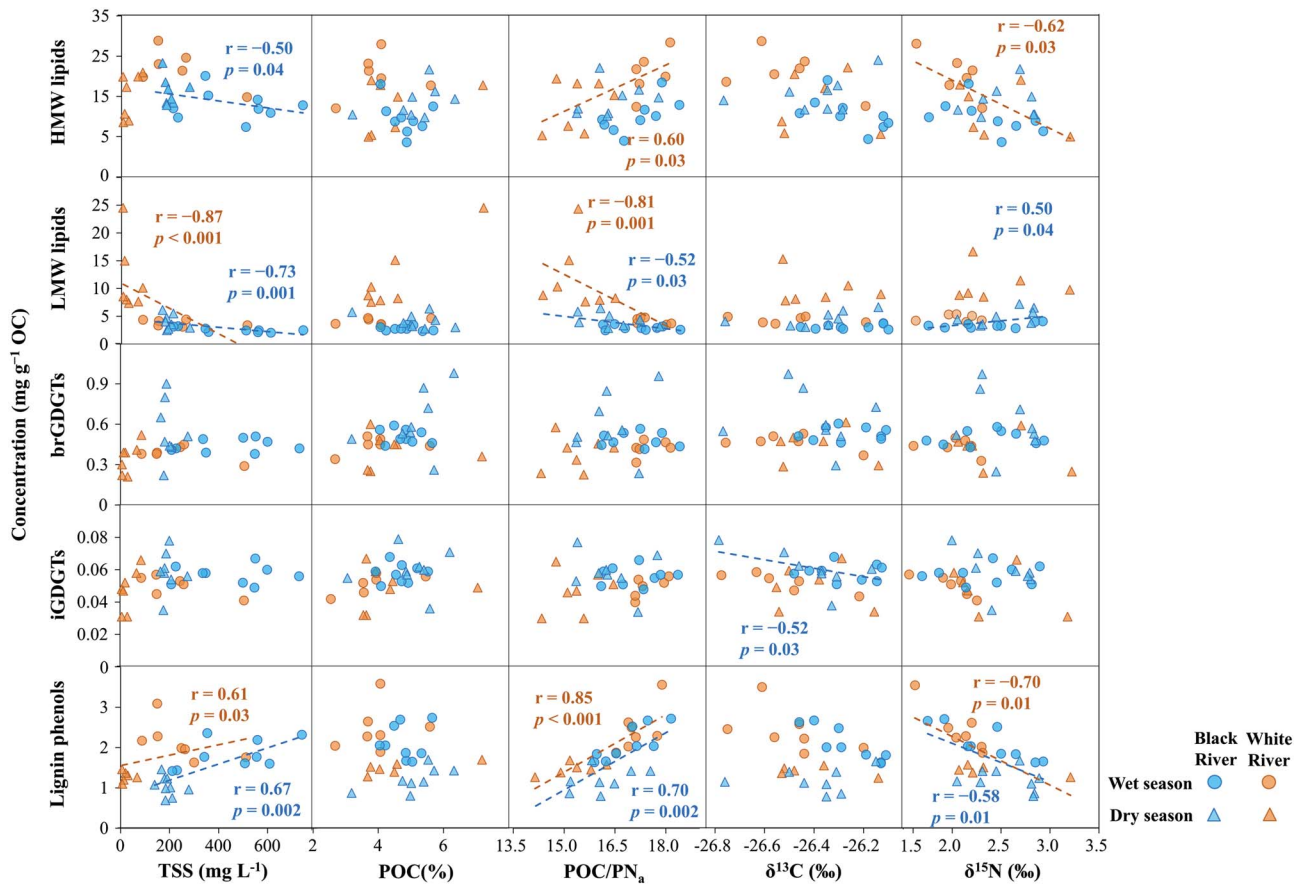
Figure 4. Relationships of the organic carbon (OC)-normalized concentrations of biomarkers in riverine particulate organic matter (POM) with river and POM properties. Blue and orange lines indicate correlations for the Black and White Rivers, respectively ($p < 0.05$). BrGDGTs = branched glycerol dialkyl glycerol tetraethers; iGDGTs = isoprenoid glycerol dialkyl glycerol tetraethers. Other abbreviations are defined in the footnote of Figure 2 and Table 1.

those typically observed for extant higher plants (>5 and >1, respectively; Cranwell et al., 1987; Bianchi & Canuel, 2011) as well as soils within each river basin (Table S2), suggesting a dominant contribution of *n*-alkanes from terrestrial sources.

Nonetheless, it should be mentioned that emergent macrophytes (such as *Batrachium bungei*, *Potamogeton crispus*, and *Potamogeton heteraculis*; Yu et al., 2017; Li, Chen, et al., 2018) are common species in the Zoige wetland, which also contributed to OC in the soil as well as riverine POM, reflected by the intermediate values of P_{aq} in soils and, to a greater extent, POM (Figure 3a; Ficken et al., 2000). LMW lipids (in particular C_{17} *n*-alkane, indicating a dominant aquatic phytoplankton source; Bianchi & Canuel, 2011; Cranwell et al., 1987) were also higher in the POM than in soils, especially in the dry season in the White River (Figure 5), likely indicating the contribution of in situ production to POM during this season. Consistently, the higher BIT values in the POM than in catchment soils (Table S2) as well as the slightly higher IR and CBT′ values in the dry- than in the wet-season POM also imply that the POM likely contains additional, river-produced 6-methyl brGDGTs during the dry season (Naeher et al., 2014). However, as shown from the constant bulk OC properties ($\delta^{13}C$ of −26.37 ± 0.03; $\delta^{15}N$ of 2.38 ± 0.07; POC/PN$_a$ of 16.4 ± 0.2), the contribution of autochthonous material from macrophytes and phytoplankton appeared to be small, similar to that in previous studies (Li, Li, et al., 2018; Liu & Liu, 2017). Hence, aquatic production, although discernable based on molecular indices, seems to be limited in general.

The botanical source of terrestrial-derived OC may be inferred from the composition of lignin phenols (Ellis et al., 2012; Hernes et al., 2017; Spencer et al., 2016). Commonly, angiosperms can be distinguished from gymnosperms based on the S/V ratios, whereas soft tissues (e.g., leaves and needles) and woody tissues can be differentiated based on the C/V ratios (Goni & Hedges, 1995; Thevenot et al., 2010).
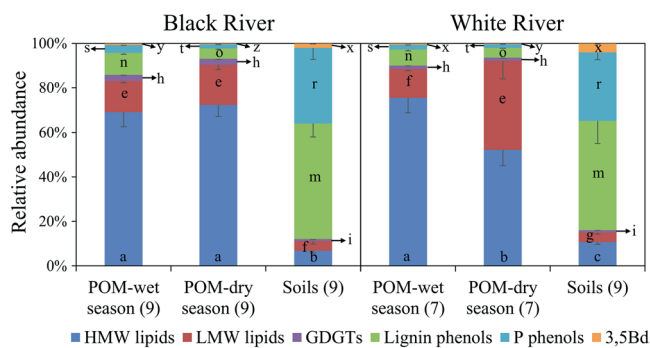
Figure 5. The relative abundance of analyzed biomarkers in riverine particulate organic matter (POM) and catchment soils of the Black and White Rivers. HMW = high molecular weight; LMW = low molecular weight; GDGTs = glycerol dialkyl glycerol tetraethers, including branched and isoprenoid GDGTs; P phenols = p-hydroxyl phenols; 3,5Bd = 3,5-dihydroxy-benzoic acid. Error bars represent standard error of the mean with the number of samples indicated in parentheses. Letters indicate different levels among POM sampled at different seasons and soils: a–c for HMW lipids, e–g for LMW lipids, h–i for GDGTs, m–o for lignin phenols, r–t for P phenols, and x–z for 3,5Bd ($p < 0.05$).

Although degradation may affect these ratios (Thevenot et al., 2010; and references therein), the high values of S/V (>1.0) and C/V (>0.9) ratios in our POM (Figure 3c and Table S2) indicate a dominance of angiosperm nonwoody tissues, consistent with the overlaying grass in the Zoige wetland. Notably, as the headstream basins of both Black and White Rivers contain areas covered by gymnosperms (such as *Abies fabri* and *Picea asperata*), the slightly higher S/V and C/V ratios (except C/V in the White River; Table S2 and Figure 3c) in the dry than in the wet season may be linked to a relatively decreased input of V phenols (from gymnosperms) from headstreams during the dry season. In addition, both P phenols and 3,5Bd are strongly and positively correlated to lignin phenols ($r > 0.8$; $p < 0.001$; $n = 18$ and 14 in the Black and White Rivers, respectively) in the Black and White River POM, suggesting similar sources of these phenols in this study. Thus, it is not surprising that the P/V and Pn/P ratios were rather constant and low for the POM (1.2 ± 0.04 and 0.09 ± 0.004 for P/V and Pn/P, respectively) and soils (1.6 ± 0.1 and 0.08 ± 0.005, respectively) in the Black and White Rivers compared to those observed for riverine organic matter from arctic basins with a high coverage of Pn-enriched *Sphagnum* (average ratios of 6.0 and 0.84, respectively; Amon et al., 2012; Tesi et al., 2014).

Although terrestrial organic matter was the primary source of POM in the Black and White Rivers, differences were observed in the composition of POM compared to that of catchment soils, best illustrated by the percentage of different compound groups in the respective matrix (Figure 5). Lignin and P phenols were the dominant compounds analyzed in the catchment soils (83% ± 2%), followed by HMW lipids (9% ± 1%). This result is consistent with biomarker distributions in the survey of alpine meadows across a much wider span on the Qinghai-Tibetan Plateau (Dai et al., 2018; Zhu et al., 2019). By comparison, HMW lipids were the most abundant (67% ± 5%) in the riverine POM, followed by LMW lipids (21% ± 5%), while lignin and P phenols only contributed to 9% ± 1% to all groups of compounds analyzed. At least two processes or factors may have contributed to the different OC composition between POM and soils. First, in contrast to lignin that is enriched in plant debris and coarse organic matter (Bergamaschi et al., 1997; Feng, Gustafsson, Holmes, Vonk, van Dongen, Semiletov, Dudarev, Yunker, Macdonald, Montluçon, et al., 2015; Feng et al., 2013), wax lipids are closely associated with mineral surfaces and preferentially stabilized in fine particles (Freymond et al., 2018). Coarse POM (>63 μm) is prone to sedimentation (i.e., settled to the sediments) during fluvial transport (Ward et al., 2013), while fine particles tend to stay longer in the surface water. Although we did not have enough POM samples for grain size measurement after all the chemical analyses, our samples collected from the surface water likely resembled fine POM (<63 μm; Hernes et al., 2017). Hydrodynamic sorting (i.e., grain-size-related physical sorting; Bianchi et al., 2007) may have contributed to the enrichment of lipids in our POM samples. Second, lignin is less hydrophobic relative to HMW lipids (Freymond et al., 2018). The low ratio of DOC/POC in the Black (0.76 ± 0.09) and White Rivers (2.70 ± 0.82) may favor the desorption of lignin from POM to DOM (Hernes et al., 2017), consistent with observations from the Andean headwaters of the Amazon River with low DOC/POC ratios (0.04 to 1.5; Hedges et al., 2000).

4.2. Seasonal Variations of POM Composition

Seasonal variation in the different molecular components of POM in the Black and White Rivers was observed for (i) their OC-normalized concentrations (Figures 2c and 2d), despite similar POC contents between seasons (Table 1), and (ii) their distinct relationships with river water or POM properties (Figure 4). First, as two groups of biomarkers for terrestrially derived organic matter, lignin phenols (in both rivers) and HMW lipids (in the White River) showed increasing concentrations with increasing ratios of POC/PN$_a$ and decreasing δ^{15}N values of POM (Figure 4). As the OC/N ratio tends to decrease with the degradation of plant-derived OC while the residues become enriched with ^{15}N due to preferential loss of ^{14}N with microbial decomposition (Kramer et al., 2017), the observed correlations reflect the decrease of HMW lipids and lignin phenols with progressive degradation of POM. However, similar to observations

made in the Mekong (Ellis et al., 2012) and Congo Rivers (Hemingway et al., 2016; Spencer et al., 2016), lignin phenols (as well as P phenols and 3,5Bd) were more concentrated in both rivers, while HMW lipids were less abundant in the Black River in the wet season (Figure 2). This contrast is reinforced by their opposite relationships with TSS in the river: While lignin phenols increase with TSS in both rivers, HMW lipids decrease in the Black River (Figure 4). Previous studies have shown that lignin is enriched in plant detritus and soil surface layers (Feng, Gustafsson, Holmes, Vonk, van Dongen, Semiletov, Dudarev, Yunker, Macdonald, Wacker, et al., 2015; Feng et al., 2013), whereas more hydrophobic HMW lipids tend to accumulate more in mineral-associated particles and subsoil horizons (Feng, Gustafsson, Holmes, Vonk, van Dongen, Semiletov, Dudarev, Yunker, Macdonald, Wacker, et al., 2015; Feng et al., 2013; Freymond et al., 2018). Hence, the intensive surface erosion and flushing of plant detritus in the wet season supplied the river with lignin-rich particles from soil surface layers (Feng et al., 2013), which diluted HMW lipids (as well as LMW lipids) in the Black River POM. In the White River, HWM lipid concentrations were comparable between seasons (Figure 2d) and not correlated to TSS, likely attributed to the low TSS concentrations in both seasons (Figure 4) that were insufficient to cause dilution effects. Alternatively, grain-size-related hydrodynamic sorting may be less intense in the wet season due to strong erosion and high water turbidity. Therefore, the enrichment of lipids (in small-sized surface POM) was less obvious in the wet season (in the Black River).

Compared to the wet-season POM, the dry-season POM was characterized by lower concentrations as well as a more variable composition of lignin phenols. First, the $(Ad/Al)_V$ and P/V (in both river) and 3,5Bd/V (in the Black River) ratios were higher in the dry than in the wet season ($p < 0.05$; Table S2 and Figures 3d and 3e), reflecting the progressive degradation of lignin during fluvial transport in the dry season (Ellis et al., 2012; Ward et al., 2013). This result is consistent with the lower POC/PN_a and CPI values in the dry- than in the wet-season POM (Tables 1 and S2), suggesting a higher degradation degree of riverine POM in the dry season. Similarly, Ward et al. (2013) estimated that about 55% of lignin fixed in the Amazonian terrestrial biosphere annually is degraded into smaller components within the river continuum. Alternatively, in the dry season, a greater proportion of POM could be derived from degraded subsoil organic matter from erosion of exposed banks compared to that in the rainy season (Feng et al., 2013; Galy et al., 2015), contributing to the higher oxidation degree of lignin phenols in the river.

LMW lipids, occurring in both aquatic and terrestrial sources (including algae, bacteria, and plants; Bianchi & Canuel, 2011; Otto & Simpson, 2005), were more concentrated in the dry season in both rivers (Figure 2), similar to observations made in the Amazon (Mortillaro et al., 2011; Saliot et al., 2001) and Orinoco Rivers (Jaffé et al., 1995). A high water transparency and low water turbidity in the dry season likely promoted in situ production and increased inputs of LMW lipids from aquatic sources. This postulation can be confirmed by the negative relationship between LMW lipids and TSS in both rivers (Figure 4). In addition, LMW lipids showed decreasing concentrations with increasing ratios of POC/PN_a in both river and decreasing $\delta^{15}N$ values of POM in the Black River, reflecting an increase of LMW lipids with progressive degradation of POM. Strong hydrodynamic sorting in low-turbidity rivers in the dry season may also contribute to the enrichment of lipids and highly oxidized organic matter with fine-sized particles in the surface water (Freymond et al., 2018; Hernes et al., 2017).

In contrast to wax lipids and lignin phenols, the OC-normalized concentrations of brGDGTs, iGDGTs, and total GDGTs were all comparable between seasons in both rivers ($p > 0.05$; Figures 2c and 2d and Table S2) and not correlated to any river water and POM properties, except for iGDGTs being negatively correlated to $\delta^{13}C$ of POM in the Black River ($p < 0.05$; Figure 4). The lack of seasonal variability in brGDGT concentrations may be associated to the supply of brGDGTs from both soils (the primary source) and in situ production within the water column (a minor source; discussed previously) and/or a much longer turnover time (~20 years) for brGDGTs (Weijers et al., 2010). Similarly, Peterse et al. (2015) found that the concentrations and relative distribution (i.e., MBT′ and CBT) of brGDGTs remained unaltered over the course of 152-day incubations of TSS from a New Zealand river. It is worth noting that no relationship existed between brGDGTs and TSS, suggesting that brGDGTs appear not associated to minerals. Given that GDGTs are hydrophobic molecules with low solubility, they are unlikely to be transported in the dissolved phase and precipitate into POM. Hence, the exact mode of transport and associations of brGDGTs with riverine POM is worth investigating in the future. In addition, the abundance of iGDGTs is negatively correlated

to the $\delta^{13}C$ of POM in the Black River ($p < 0.05$), primarily caused by the negative relationship between GDGT-0 and $\delta^{13}C$ in POM ($r = -0.51$; $p = 0.04$; $n = 18$), since GDGT-0 was the most abundant iGDGT (>80% of total iGDGTs; Figure S3b) in the riverine POM. Notably, GDGT-0/crenarchaeol ratios in POM (6.8−21) were higher than 2, suggesting GDGT-0 (i.e., iGDGTs) was mainly produced by methanogens in our river systems (Blaga et al., 2009). Methanogens produce methane that is highly depleted in ^{13}C (Hinrichs et al., 1999), which may be utilized by methanotrophic microbes, contributing to the depletion of $\delta^{13}C$ in the bulk POM and/or soils (Hollander & Smith, 2001; Naeher et al., 2014). Hence, this relationship between iGDGT and GDGT-0 abundances and POC-$\delta^{13}C$ may reflect the influence of methanogens in the carbon source of the Black River POM.

4.3. Comparison to Other River Basins

To compare with other rivers around the world, we compiled a database with both lignin phenols and wax lipids (with FAs being the most commonly analyzed component) measured for riverine POM or sediments (Figure 5). The concentration of biomarkers was normalized against the respective OC content of sample matrix (Figure 5), and the ratio of HMW FAs/lignin phenols was calculated to compare the behavior of these two groups of higher plant biomarkers. We ascertained that FAs and lignin phenols were extracted from the same batch of samples or similar sampling locations and time (for the Amazon and Congo Rivers) in the literature, including POM from the Congo (Hemingway et al., 2016; Spencer et al., 2016) and Mackenzie Rivers (Vonk et al., 2016), fine (<63 μm) or surface water POM in the lower reaches of the Amazon River and its tributaries (including Negro, Solimoes, Madeira, and Tapajós Rivers; Hedges et al., 1986; Saliot et al., 2001; Ward et al., 2013), and surface sediments in the Danube (Freymond et al., 2018), the lower reaches of Yangtze (Li et al., 2015; Ma et al., 2015), and Arctic Rivers (including Kolyma, Indigirka, Lena, Yenisey, Ob, and Kalix Rivers; Feng et al., 2013; van Dongen et al., 2008).

Compared with those in the other rivers, the OC-normalized concentrations of lignin phenols are significantly lower in the Black and White Rivers, while terrestrial plant-derived HMW FAs are much higher (Figure 6). The ratios of HWM FAs/lignin phenols were 5.1 ± 0.6 and 5.4 ± 0.5 in the Black and White Rivers, respectively, about 2 orders of magnitude higher than those of other rivers (Figure 6). Given the coarse texture of soils across the Qinghai-Tibetan Plateau (partly related to the low weathering state of parent materials; Baumann et al., 2009), POM is unlikely to receive large amounts of fine-sized particles in our studied rivers, especially compared to some of the highly weathered catchments with clayey soils (such as the Amazon). Furthermore, POM in this study is highly enriched in HMW FAs even compared with fine (<63 μm) or surface water POM in the lower reaches of the Amazon River (Hedges et al., 1986; Saliot et al., 2001; Ward et al., 2013). Hence, we do not think that this contrast is related to the grain size of POM. Instead, the distinct biomarker composition suggests different carbon sources for the Zoige-draining rivers versus other rivers around the world.

The vegetation of the Black and White River basins is dominated by grasses (coverage up to 90%; Ma et al., 2016), while the catchments of the Congo, Amazon, Yangtze, and Arctic Rivers are largely characterized by forests (>60%), with grassland comprising <20% of the basin area (Amon et al., 2012; Feng, Gustafsson, Holmes, Vonk, van Dongen, Semiletov, Dudarev, Yunker, Macdonald, Montluçon, et al., 2015; Hemingway et al., 2016; van Dongen et al., 2008). These results are consistent with the higher S/V and C/V ratios in the Black and White River POM (average S/V = 1.20 ± 0.04 and C/V = 0.97 ± 0.04; Table S2) than those in other rivers analyzed in this study (S/V = 0.64 ± 0.05 and C/V = 0.15 ± 0.02), supporting a predominance of herbaceous rather than woody plants in our study area. Thus, we postulate that the high ratio of HWM FAs/lignin phenols in the Black and White River POM resulted from the lower abundance of lignin and higher abundance of wax lipids in grass tissues compared with those in woody counterparts (Ishiwatari et al., 2006; Moingt et al., 2016). In support of this postulation, previous studies showed that lignin contents of herbaceous plants are 2–3 times lower than those in woody plants (angiosperms and gymnosperms; Jacquemoud et al., 1995) and that HMW FAs are the predominant lipid components of herbs (Ishiwatari et al., 2006). Similarly, Moingt et al. (2016) found that the lignin phenols were approximately 3 times lower in the nonwoody (leaves) than in the woody parts of angiosperms (e.g., *Betula papyrifera*, *populous tremuloides, Acer saccharum*), while wax lipid contents were 3.5 times higher in wheat leaves than in stems (Wiesenberg et al., 2010). Hence, for the Black and White Rivers draining grass-dominated wetlands, wax lipids rather than lignin constitute a higher proportion of
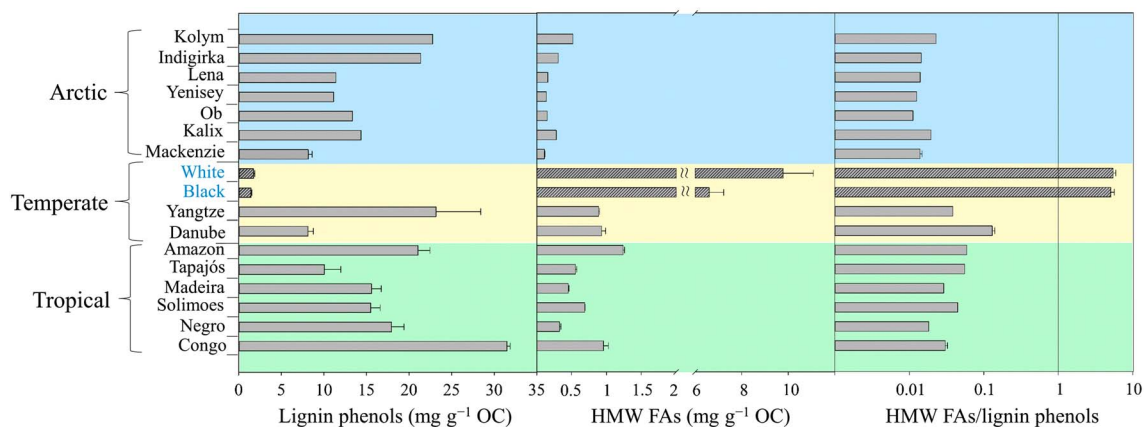
Figure 6. Comparison of the abundance of lignin phenols, high-molecular-weight (HMW) fatty acids (FAs), and the ratios of HMW FAs/lignin phenols in the particulate organic matter (POM) of the Black and White Rivers to those in the POM or sediments of Arctic, temperate, and tropical rivers. Original data are found in Feng et al. (2013) for lignin phenols and van Dongen et al. (2008) for HMW FAs in sediments of Arctic rivers (Kolyma, Indigirka, Lena, Yenisey, Ob, and Kalix Rivers), Vonk et al. (2016) for both lignin phenols and HMW FAs in POM (>0.7 μm) of the Mackenzie River, Li et al. (2015) for lignin phenols and Ma et al. (2015) for HMW FAs in sediments of the lower reaches of Yangtze River, Freymond et al. (2018) for both lignin phenols and HMW FAs in sediments of the Danube River, Hedges et al. (1986) for lignin phenols in fine POM (<63 μm) and Saliot et al. (2001) for HMW FAs in POM (>0.7 μm) of tropical rivers (Negro, Solimoes, Madeira, Tapajós, and Amazon Rivers), and Spencer et al. (2016) for lignin phenols and Hemingway et al. (2016) for HMW FAs in POM (>0.7 μm) of the Congo River.

terrestrial organic matter exported. In addition, a better preservation of lipids in wetland soils is suggested compared with that in oxic upland soils due to thermodynamic constraints on the anaerobic decomposition of reduced compounds (Keiluweit et al., 2017), which may also contribute to the observed compositional difference in POM from wetland-draining versus large rivers.

5. Conclusions

This study presents the first molecular investigation on the composition of fluvial POM exported from Zoige wetland, the world's largest alpine peat wetland located in northeastern Qinghai-Tibetan Plateau. Both biomarkers and bulk properties indicate a predominant terrestrial origin of POM in the Black and White Rivers. However, compositional differences were also observed between POM and soils: While lignin and P phenols were the dominant compounds analyzed in the catchment soils ($83\% \pm 2\%$), HMW lipids were the most abundant ($67\% \pm 5\%$) in the riverine POM, likely attributed to the differential influences from abiotic processes (i.e., hydrodynamic sorting and dissolution). Distinct behavior was observed for different molecular components of POM in the Black and White Rivers. Lignin phenols were more concentrated in the wet season in both rivers, while HMW lipids were less abundant in the Black River. Along with their opposite relationships with TSS, these results indicate an enhanced input of lignin-rich particles from soil surface layers in the wet season, which diluted HMW lipids (as well as LMW lipids) in the Black River POM. In the White River, the low TSS concentrations in both seasons were insufficient to cause dilution effects. By comparison, brGDGTs show minimal response to seasonal changes in hydrological regimes. Compared to that of other rivers around the world with a higher coverage of forests in the basin, the much higher ratio of HMW FAs/lignin phenols in the Black and White Rivers can be attributed to the lower lignin content in the grass relative to woody species and/or molecular characteristics in the wetland soils. Our study provides benchmark information on compositional characteristics of fluvial POM exported from the Zoige wetland and highlights the divergent behavior of molecular components during fluvial transfer. Such information is vital for assessing future changes in the Zoige wetland, given its high vulnerability to climatic and land use changes.

References

Amon, R. M. W., Rinehart, A. J., Duan, S., Louchouarn, P., Prokushkin, A., Guggenberger, G., et al. (2012). Dissolved organic matter sources in large Arctic rivers. *Geochimica et Cosmochimica Acta*, *94*, 217–237. https://doi.org/10.1016/j.gca.2012.07.015

Annual Hydrological Report P.R. China (2015). Hydrological data of Yellow River basin. No. 1, Upper Reaches of the Yellow River (above the Heishan Gorge). *Bureau of Hydrology, Ministry of Water Resources, P.R. China*. (In Chinese).

Baumann, F., He, J.-S., Schmidt, K., Kuehn, P., & Scholten, T. (2009). Pedogenesis, permafrost, and soil moisture as controlling factors for soil nitrogen and carbon contents across the Tibetan Plateau. *Global Change Biology*, *15*(12), 3001–3017. https://doi.org/10.1111/j.1365-2486.2009.01953.x

Bergamaschi, B. A., Tsamakis, E., Keil, R. G., Eglinton, T. I., Montluçon, D. B., & Hedges, J. I. (1997). The effect of grain size and surface area on organic matter, lignin and carbohydrate concentration, and molecular compositions in Peru Margin sediments. *Geochimica et Cosmochimica Acta*, *61*(6), 1247–1260. https://doi.org/10.1016/S0016-7037(96)00394-8

Bianchi, T. S., & Canuel, E. A. (2011). *Chemical Biomarkers in Aquatic Ecosystems*. Princeton (NJ): Princeton University Press.

Bianchi, T. S., Galler, J. J., & Allison, M. A. (2007). Hydrodynamic sorting and transport of terrestrially derived organic carbon in sediments of the Mississippi and Atchafalaya Rivers. *Estuarine, Coastal and Shelf Science*, *73*(1-2), 211–222. https://doi.org/10.1016/j.ecss.2007.01.004

Blaga, C. I., Reichart, G. J., Heiri, O., & Sinninghe Damsté, J. S. (2009). Tetraether membrane lipid distributions in water-column particulate matter and sediments: A study of 47 European lakes along a north–south transect. *Journal of Paleolimnology*, *41*(3), 523–540. https://doi.org/10.1007/s10933-008-9242-2

Cole, J. J., Prairie, Y. T., Caraco, N. F., McDowell, W. H., Tranvik, L. J., Striegl, R. G., et al. (2007). Plumbing the global carbon cycle: Integrating inland waters into the terrestrial carbon budget. *Ecosystems*, *10*(1), 172–185. https://doi.org/10.1007/s10021-006-9013-8

Cranwell, P. A., Eglinton, G., & Robinson, N. (1987). Lipids of aquatic organisms as potential contributors to lacustrine sediments—II. *Organic Geochemistry*, *11*(6), 513–527. https://doi.org/10.1016/0146-6380(87)90007-6

Dai, G., Ma, T., Zhu, S., Liu, Z., Chen, D., Bai, Y., et al. (2018). Large-scale distribution of molecular components in Chinese grassland soils: The influence of input and decomposition processes. *Journal of Geophysical Research: Biogeosciences*, *123*(1), 239–255. https://doi.org/10.1002/2017JG004233

Dang, X., Yang, H., Naafs, B. D. A., Pancost, R. D., & Xie, S. (2016). Evidence of moisture control on the methylation of branched glycerol dialkyl glycerol tetraethers in semi-arid and arid soils. *Geochimica et Cosmochimica Acta*, *189*, 24–36. https://doi.org/10.1016/j.gca.2016.06.004

De Jonge, C., Stadnitskaia, A., Hopmans, E. C., Cherkashov, G., Fedotov, A., & Sinninghe Damsté, J. S. (2014). In situ produced branched glycerol dialkyl glycerol tetraethers in suspended particulate matter from the Yenisei River, Eastern Siberia. *Geochimica et Cosmochimica Acta*, *125*, 476–491. https://doi.org/10.1016/j.gca.2013.10.031

Ellis, E. E., Keil, R. G., Ingalls, A. E., Richey, J. E., & Alin, S. R. (2012). Seasonal variability in the sources of particulate organic matter of the Mekong River as discerned by elemental and lignin analyses. *Journal of Geophysical Research*, *117*, G01038. https://doi.org/10.1029/2011JG001816

Feng, X., Gustafsson, Ö., Holmes, R. M., Vonk, J. E., van Dongen, B. E., Semiletov, I. P., et al. (2015). Multi-molecular tracers of terrestrial carbon transfer across the pan-Arctic: comparison of hydrolyzable components with plant wax lipids and lignin phenols. *Biogeosciences*, *12*(15), 4841–4860. https://doi.org/10.5194/bg-12-4841-2015

Feng, X., Gustafsson, Ö., Holmes, R. M., Vonk, J. E., van Dongen, B. E., Semiletov, I. P., et al. (2015). Multimolecular tracers of terrestrial carbon transfer across the pan-Arctic: [14]C characteristics of sedimentary carbon components and their environmental controls. *Global Biogeochemical Cycles*, *29*, 1855–1873. https://doi.org/10.1002/2015GB005204

Feng, X., Vonk, J. E., van Dongen, B. E., Gustafsson, Ö., Semiletov, I. P., Dudarev, O. V., et al. (2013). Differential mobilization of terrestrial carbon pools in Eurasian Arctic river basins. *Proceedings of the National Academy of Sciences of the United States of America*, *110*, 14,168–14,173. https://doi.org/10.1073/pnas.1307031110

Ficken, K. J., Li, B., Swain, D. L., & Eglinton, G. (2000). An *n*-alkane proxy for the sedimentary input of submerged/floating freshwater aquatic macrophytes. *Organic Geochemistry*, *31*(7-8), 745–749. https://doi.org/10.1016/S0146-6380(00)00081-4

Freymond, C. V., Kündig, N., Stark, C., Peterse, F., Buggle, B., Lupker, M., et al. (2018). Evolution of biomolecular loadings along a major river system. *Geochimica et Cosmochimica Acta*, *223*, 389–404. https://doi.org/10.1016/j.gca.2017.12.010

Galy, V., Peucker-Ehrenbrink, B., & Eglinton, T. (2015). Global carbon export from the terrestrial biosphere controlled by erosion. *Nature*, *521*(7551), 204–207. https://doi.org/10.1038/nature14400

Gao, J., Lei, G., Zhang, X., & Wang, G. (2014). Can δ^{13}C abundance, water-soluble carbon, and light fraction carbon be potential indicators of soil organic carbon dynamics in Zoigê wetland? *Catena*, *119*, 21–27. https://doi.org/10.1016/j.catena.2014.03.005

Goni, M. A., & Hedges, J. I. (1995). Sources and reactivities of marine-derived organic matter in coastal sediments as determined by alkaline CuO oxidation. *Geochimica et Cosmochimica Acta*, *59*(14), 2965–2981. https://doi.org/10.1016/0016-7037(95)00188-3

Hedges, J. I., Clark, W. A., Quay, P. D., Richey, J. E., Devol, A. H., & Santos, U. D. (1986). Composition and fluxes of particulate organic material in the Amazon River. *Limnology and Oceanography*, *31*(4), 717–738. https://doi.org/10.4319/lo.1986.31.4.0717

Hedges, J. I., Mayorga, E., Tsamakis, E., McClain, M. E., Aufdenkampe, A., Quay, P., et al. (2000). Organic matter in Bolivian tributaries of the Amazon River: A comparison to the lower mainstream. *Limnology and Oceanography*, *45*(7), 1449–1466. https://doi.org/10.4319/lo.2000.45.7.1449

Hemingway, J. D., Schefuß, E., Dinga, B. J., Pryer, H., & Galy, V. V. (2016). Multiple plant-wax compounds record differential sources and ecosystem structure in large river catchments. *Geochimica et Cosmochimica Acta*, *184*, 20–40. https://doi.org/10.1016/j.gca.2016.04.003

Hemingway, J. D., Schefuß, E., Spencer, R. G. M., Dinga, B. J., Eglinton, T. I., McIntyre, C., & Galy, V. V. (2017). Hydrologic controls on seasonal and inter-annual variability of Congo River particulate organic matter source and reservoir age. *Chemical Geology*, *466*, 454–465. https://doi.org/10.1016/j.chemgeo.2017.06.034

Hernes, P. J., Dyda, R. Y., & McDowell, W. H. (2017). Connecting tropical river DOM and POM to the landscape with lignin. *Geochimica et Cosmochimica Acta*, *219*, 143–159. https://doi.org/10.1016/j.gca.2017.09.028

Hinrichs, K. U., Hayes, J. M., Sylva, S. P., Brewer, P. G., & DeLong, E. F. (1999). Methane-consuming archaebacteria in marine sediments. *Nature*, *398*(6730), 802–805. https://doi.org/10.1038/19751

Hollander, D. J., & Smith, M. A. (2001). Microbially mediated carbon cycling as a control on the δ^{13}C of sedimentary carbon in eutrophic Lake Mendota (USA): New models for interpreting isotopic excursions in the sedimentary record. *Geochimica et Cosmochimica Acta*, *65*(23), 4321–4337. https://doi.org/10.1016/S0016-7037(00)00506-8

Hopmans, E. C., Schouten, S., & Sinninghe Damsté, J. S. (2016). The effect of improved chromatography on GDGT-based palaeoproxies. *Organic Geochemistry*, *93*, 1–6. https://doi.org/10.1016/j.orggeochem.2015.12.006

Hopmans, E. C., Weijers, J. W. H., Schefuß, E., Herfort, L., Sinninghe Damsté, J. S., & Schouten, S. (2004). A novel proxy for terrestrial organic matter in sediments based on branched and isoprenoid tetraether lipids. *Earth and Planetary Science Letters*, *224*(1-2), 107–116. https://doi.org/10.1016/j.epsl.2004.05.012

Huguet, C., Hopmans, E. C., Febo-Ayala, W., Thompson, D. H., Sinninghe Damsté, J. S., & Schouten, S. (2006). An improved method to determine the absolute abundance of glycerol dibiphytanyl glycerol tetraether lipids. *Organic Geochemistry*, *37*(9), 1036–1041. https://doi.org/10.1016/j.orggeochem.2006.05.008

Huotari, J., Nykänen, H., Forsius, M., & Arvola, L. (2013). Effect of catchment characteristics on aquatic carbon export from a boreal catchment and its importance in regional carbon cycling. *Global Change Biology*, *19*(12), 3607–3620. https://doi.org/10.1111/gcb.12333

Ihejirika, C. E., Njoku, J. D., Ujowundu, C. O., Onwudike, S. U., & Uzoka, C. N. (2011). Synergism between season, pH, conductivity and total dissolved solids (TDS) of Imo River quality for agricultural irrigation. *Journal of Biodiversity and Environmental Sciences*, *1*, 26–31.

International Union of Soil Sciences Working Group World Reference Base (2015). World reference base for soil resources 2014, update 2015. World soil resources reports, No. 106. FAO, Rome.

Ishiwatari, R., Yamamoto, S., & Shinoyama, S. (2006). Lignin and fatty acid records in Lake Baikal sediments over the last 130 kyr: A comparison with pollen records. *Organic Geochemistry*, *37*(12), 1787–1802. https://doi.org/10.1016/j.orggeochem.2006.10.005

Jacquemoud, S., Verdebout, J., Schmuck, G., Andreoli, G., & Hosgood, B. (1995). Investigation of leaf biochemistry by statistics. *Remote Sensing of Environment*, *54*(3), 180–188. https://doi.org/10.1016/0034-4257(95)00170-0

Jaffé, R., Rushdi, A. I., Medeiros, P. M., & Simoneit, B. R. T. (2006). Natural product biomarkers as indicators of sources and transport of sedimentary organic matter in a subtropical river. *Chemosphere*, *64*(11), 1870–1884. https://doi.org/10.1016/j.chemosphere.2006.01.048

Jaffé, R., Wolff, G. A., Cabrera, A. C., & Chitty, H. C. (1995). The biogeochemistry of lipids in rivers of the Orinoco Basin. *Geochimica et Cosmochimica Acta*, *59*(21), 4507–4522. https://doi.org/10.1016/0016-7037(95)00246-V

Keiluweit, M., Wanzek, T., Kleber, M., Nico, P., & Fendorf, S. (2017). Anaerobic microsites have an unaccounted role in soil carbon stabilization. *Nature Communications*, *8*(1), 1771. https://doi.org/10.1038/s41467-017-01406-6

Kramer, M. G., Lajtha, K., & Aufdenkampe, A. K. (2017). Depth trends of soil organic matter C:N and ^{15}N natural abundance controlled by association with minerals. *Biogeochemistry*, *136*(3), 237–248. https://doi.org/10.1007/s10533-017-0378-x

Li, B., Chen, F., Xu, D., Wang, Z., & Tao, M. (2018). Trophic interactions in the Zoige alpine wetland on the eastern edge of the Qinghai-Tibetan Plateau inferred by stable isotopes. *Limnology*, *19*(3), 285–297. https://doi.org/10.1007/s10201-018-0546-2

Li, G., Li, L., Tarozo, R., Longo, W. M., Wang, K. J., Dong, H., & Huang, Y. (2018). Microbial production of long-chain *n*-alkanes: Implication for interpreting sedimentary leaf wax signals. *Organic Geochemistry*, *115*, 24–31. https://doi.org/10.1016/j.orggeochem.2017.10.005

Li, Z., Peterse, F., Wu, Y., Bao, H., Eglinton, T. I., & Zhang, J. (2015). Sources of organic matter in Changjiang (Yangtze River) bed sediments: Preliminary insights from organic geochemical proxies. *Organic Geochemistry*, *85*, 11–21. https://doi.org/10.1016/j.orggeochem.2015.04.006

Limpens, J., Berendse, F., Blodau, C., Canadell, J. G., Freeman, C., Holden, J., et al. (2008). Peatlands and the carbon cycle: From local processes to global implications—A synthesis. *Biogeosciences*, *5*(5), 1475–1491. https://doi.org/10.5194/bg-5-1475-2008

Liu, H., & Liu, W. (2017). Concentration and distributions of fatty acids in algae, submerged plants and terrestrial plants from the northeastern Tibetan Plateau. *Organic Geochemistry*, *113*, 17–26. https://doi.org/10.1016/j.orggeochem.2017.08.008

Ma, K., Zhang, Y., Tang, S., & Liu, J. (2016). Spatial distribution of soil organic carbon in the Zoige alpine wetland, northeastern Qinghai-Tibet Plateau. *Catena*, *144*, 102–108. https://doi.org/10.1016/j.catena.2016.05.014

Ma, Q., Wei, X., Wu, Y., & Zhang, J. (2015). Composition and distribution of organic matter in the surface sediments of the Changjiang River in post-Three Gorges Dam period. *China Environmental Science*, *35*(8), 2485–2493. (In Chinese)

Ma, T., Dai, G., Zhu, S., Chen, D., Chen, L., Lü, X., et al. (2019). Distribution and preservation of root- and shoot-derived carbon components in soils across the Chinese-Mongolian grasslands. *Journal of Geophysical Research: Biogeosciences*, *124*(2), 420–431. https://doi.org/10.1029/2018jg004915

McClelland, J. W., Holmes, R. M., Peterson, B. J., Raymond, P. A., Striegl, R. G., Zhulidov, A. V., et al. (2016). Particulate organic carbon and nitrogen export from major Arctic rivers. *Global Biogeochemical Cycles*, *30*, 629–643. https://doi.org/10.1002/2015GB005351

Moingt, M., Lucotte, M., & Paquet, S. (2016). Lignin biomarkers signatures of common plants and soils of Eastern Canada. *Biogeochemistry*, *129*(1-2), 133–148. https://doi.org/10.1007/s10533-016-0223-7

Mortillaro, J. M., Abril, G., Moreira-Turcq, P., Sobrinho, R. L., Perez, M., & Meziane, T. (2011). Fatty acid and stable isotope (δ^{13}C, δ^{15}N) signatures of particulate organic matter in the lower Amazon River: Seasonal contrasts and connectivity between floodplain lakes and the mainstem. *Organic Geochemistry*, *42*(10), 1159–1168. https://doi.org/10.1016/j.orggeochem.2011.08.011

Naeher, S., Peterse, F., Smittenberg, R. H., Niemann, H., Zigah, P. K., & Schubert, C. J. (2014). Sources of glycerol dialkyl glycerol tetraethers (GDGTs) in catchment soils, water column and sediments of Lake Rotsee (Switzerland)—Implications for the application of GDGT-based proxies for lakes. *Organic Geochemistry*, *66*, 164–173. https://doi.org/10.1016/j.orggeochem.2013.10.017

Otto, A., & Simpson, M. J. (2005). Degradation and preservation of vascular plant-derived biomarkers in grassland and forest soils from western Canada. *Biogeochemistry*, *74*(3), 377–409. https://doi.org/10.1007/s10533-004-5834-8

Patwardhan, A. P., & Thompson, D. H. (1999). Efficient synthesis of 40-and 48-membered tetraether macrocyclic bisphosphocholines. *Organic Letters*, *1*(2), 241–244. https://doi.org/10.1021/ol990567o

Pawson, R. R., Lord, D. R., Evans, M. G., & Allott, T. E. H. (2008). Fluvial organic carbon flux from an eroding peatland catchment, southern Pennines, UK. *Hydrology and Earth System Sciences*, *12*(2), 625–634. https://doi.org/10.5194/hess-12-625-2008

Peterse, F., Moy, C. M., & Eglinton, T. I. (2015). A laboratory experiment on the behaviour of soil-derived core and intact polar GDGTs in aquatic environments. *Biogeosciences*, *12*(4), 933–943. https://doi.org/10.5194/bg-12-933-2015

Regnier, P., Friedlingstein, P., Ciais, P., Mackenzie, F. T., Gruber, N., Janssens, I. A., et al. (2013). Anthropogenic perturbation of the carbon fluxes from land to ocean. *Nature Geoscience*, *6*(8), 597–607. https://doi.org/10.1038/ngeo1830

Saliot, A., Mejanelle, L., Scribe, P., Fillaux, J., Pepe, C., Jabaud, A., & Dagaut, J. (2001). Particulate organic carbon, sterols, fatty acids and pigments in the Amazon River system. *Biogeochemistry*, *53*(1), 79–103. https://doi.org/10.1023/A:1010754022594

Schlünz, B., & Schneider, R. R. (2000). Transport of terrestrial organic carbon to the oceans by rivers: Re-estimating flux- and burial rates. *International Journal of Earth Sciences*, *88*(4), 599–606. https://doi.org/10.1007/s005310050290

Schouten, S., Hopmans, E. C., & Sinninghe Damsté, J. S. (2013). The organic geochemistry of glycerol dialkyl glycerol tetraether lipids: A review. *Organic Geochemistry*, *54*, 19–61. https://doi.org/10.1016/j.orggeochem.2012.09.006

Spencer, R. G. M., Hernes, P. J., Dinga, B., Wabakanghanzi, J. N., Drake, T. W., & Six, J. (2016). Origins, seasonality, and fluxes of organic matter in the Congo River. *Global Biogeochemical Cycles*, *30*, 1105–1121. https://doi.org/10.1002/2016gb005427

Tesi, T., Semiletov, I., Hugelius, G., Dudarev, O., Kuhry, P., & Gustafsson, Ö. (2014). Composition and fate of terrigenous organic matter along the Arctic land–ocean continuum in East Siberia: Insights from biomarkers and carbon isotopes. *Geochimica et Cosmochimica Acta*, *133*, 235–256. https://doi.org/10.1016/j.gca.2014.02.045

Thevenot, M., Dignac, M.-F., & Rumpel, C. (2010). Fate of lignins in soils: A review. *Soil Biology and Biochemistry*, *42*(8), 1200–1211. https://doi.org/10.1016/j.soilbio.2010.03.017

van Dongen, B. E., Semiletov, I., Weijers, J. W. H., & Gustafsson, O. (2008). Contrasting lipid biomarker composition of terrestrial organic matter exported from across the Eurasian Arctic by the five great Russian Arctic rivers. *Global Biogeochemical Cycles*, *22*, GB1011. https://doi.org/10.1029/2007GB002974

Vonk, J. E., Dickens, A. F., Giosan, L., Hussain, Z. A., Kim, B., Zipper, S. C., et al. (2016). Arctic deltaic lake sediments as recorders of fluvial organic matter deposition. *Frontiers in Earth Science*, *4*, 77. https://doi.org/10.3389/feart.2016.00077

Wang, Y., Wang, X., & Yang, Z. (2010). Water resources variation in Zoige wetland and causes analysis. *Proceedings of Conference on Environmental Pollution and Public Health*, *5*, 1392–1396. (In Chinese)

Ward, N. D., Keil, R. G., Medeiros, P. M., Brito, D. C., Cunha, A. C., Dittmar, T., et al. (2013). Degradation of terrestrially derived macromolecules in the Amazon River. *Nature Geoscience*, *6*(7), 530–533. https://doi.org/10.1038/ngeo1817

Weijers, J. W. H., Wiesenberg, G. L. B., Bol, R., Hopmans, E. C., & Pancost, R. D. (2010). Carbon isotopic composition of branched tetraether membrane lipids in soils suggest a rapid turnover and a heterotrophic life style of their source organism(s). *Biogeosciences*, *7*(9), 2959–2973. https://doi.org/10.5194/bg-7-2959-2010

Wiesenberg, G. L. B., Dorodnikov, M., & Kuzyakov, Y. (2010). Source determination of lipids in bulk soil and soil density fractions after four years of wheat cropping. *Geoderma*, *156*(3-4), 267–277. https://doi.org/10.1016/j.geoderma.2010.02.026

Worrall, F., Moody, C. S., Clay, G. D., Burt, T. P., & Rose, R. (2017). The flux of organic matter through a peatland ecosystem: The role of cellulose, lignin, and their control of the ecosystem oxidation state. *Journal of Geophysical Research: Biogeosciences*, *122*, 1655–1671. https://doi.org/10.1002/2016jg003697

Yang, G., Wang, M., Chen, H., Liu, L., Wu, N., Zhu, D., et al. (2017). Responses of CO_2 emission and pore water DOC concentration to soil warming and water table drawdown in Zoige Peatlands. *Atmospheric Environment*, *152*, 323–329. https://doi.org/10.1016/j.atmosenv.2016.12.051

Yu, J., Wu, Z., Zhou, J., Huang, J., & Chen, F. (2017). Studies on the diversity of aquatic plants in Zoige Plateau wetland. *Journal of Wuhan University (Natural Science Edition)*, *63*(1), 86–94. (In Chinese)

Zhou, W., Suolang, D., Cui, L., Wang, Y., & Li, W. (2015). Effects of fencing and grazing on the emissions of CO_2 and CH_4 in Zoige Peatland, East Qinghai-Tibetan Plateau. *Ecology and Environmental Sciences*, *24*, 183–189. (In Chinese)

Zhu, D., Wu, N., Chen, H., Zhu, Q., Wu, Y., & Zhang, Y. (2014). Spatial pattern of dissolved organic carbon and its specific ultraviolet absorbance under different scales in a wetland complex on the Eastern Tibetan Plateau. *Ekoloji*, *23*, 16–21. https://doi.org/10.5053/ekoloji.2014.913

Zhu, S., Dai, G., Ma, T., Chen, L., Chen, D., Lü, X., et al. (2019). Distribution of lignin phenols in comparison with plant-derived lipids in the alpine versus temperate grassland soils. *Plant and Soil*, *439*(1-2), 325–338. https://doi.org/10.1007/s11104-019-04035-8